Thermochimica Acta, 153 (1989) 349–417
Elsevier Science Publishers B.V., Amsterdam – Printed in The Netherlands

Review

NONEQUILIBRIUM PROCESSES OF MELT SOLIDIFICATION DURING PROGRAMMED TEMPERATURE CHANGES AND THE METASTABLE PHASES FORMATION

Z. CHVOJ, Z. KOŽÍŠEK and J. ŠESTÁK

Institute of Physics, Czechoslovak Academy of Science, Na Slovance 2, 18040 Praha 8 (Czechoslovakia)

(Received 10 February 1988)

CONTENTS

I. INTRODUCTION

Firing of substances is one of the basic methods of preparing materials having defined properties (see Table 1). It follows that a programmed change of temperature is applied not only in nature but also in many modern techniques, furnishing the basis of almost all technically important materials from single crystals up to glasses. In order to define such materials we need to know (besides their structure) their thermodynamic behaviour, i.e. stability of each state, phase relations and characteristic temperatures of phase transformations. All this can be found in ordinary thermodynamics

0040-6031/89/$03.50

TABLE 1

The rate of temperature changes as a decisive parameter for material formation in different states of stability

Cooling rate	Type of process	Type of material	Method of formation
$<10^{-10}$	Infinitely slow crystallization	Minerals, single crystals	Geological processes
10^{-7} to 10^{-4}	Controlled crystallization	Natural and synthetic single crystals	Crystal growth from solutions, gels and coarsening of solids
10^{-1}	Thermophysical measurements		
10^{2}	Ordinary cooling	Oxides, silicates and chalcogenides	Casting, immersion
10^{5} to 10^{8}	Freeze-in by ultrafast cooling	Metals and other materials	Melt splatting or spinning techniques
10^{11}	Disordering on surfaces	Layers on metallic and other materials	Vapor deposition or laser glasing

(dealt with in a large number of textbooks); as a matter of fact it is a "thermostatic" description employing a conventional form of equilibrium phase diagrams. Tabulated phase diagrams have become important assistants in the preparation of ceramic materials [1], particularly oxide systems, and have been regularly published since 1964 by the American Ceramic Society. It is worth noting that reference data gradually has revealed a series of changes reflecting the amount of heating required to achieve equilibrium, e.g. in the SiO_2–Al_2O_3 system, the process of melting changes from eutectic to peritectic in character, whilst lengthening the equilibration time from hours to weeks [1]. From Table 1 it is evident that conditions which are extremely close to actual equilibrium are only possible to reach with very slow cooling and/or heating, such as is regularly achievable only during geological processes. Actually-available rates of thermophysical measurements [2,3] fall, however, in the boundary area of so-called thermodynamically extreme conditions of rapid heating and/or cooling. Introduction of real conditions to the existing thermophysical description is herewith the subject of our review.

In the classical thermodynamic description of a system in chemical equilibrium, the given phase areas in a phase diagram represent zones of minima of the Gibbs energy G, and the phase coexistence is given by the Gibbs phase rule. To construct a phase diagram requires mapping all available phases and locating their phase boundaries. This is, unfortunately, not possible simply by direct measurements of temperature and/or concentration dependences of ΔG. If the measurement of electromotive force E is possible, ΔG for the reaction is available by means of the direct proportionality $\Delta G = m\mathcal{F}E$ (where m and $\mathcal{F}$ are the charge and the Faraday

constant respectively). This method is of course only useful in the case of a suitable reversible cell, e.g. in alkali metal chloride systems [4], where it serves to give straightforward estimates of the stability and the metastability of a given substance by indicating positive and negative changes in ΔG respectively. Another method of estimating ΔG is by means of enthalpy changes ΔH, using the Gibbs–Helmholtz equation $\Delta G = \Delta H - T\Delta S$. This falls within the broad scope of calorimetry and thus the calorimeter is extremely important to the versatile thermochemist (see refs. 5 and 6 (monographs) and refs. 7–10 (review articles), and also refs. 11–14 which include applications to the thermochemistry of alloys).

The classification of calorimeters is usually based on three main variables. These are heat produced or absorbed Q, temperature of the sample T_s (i.e. that of the entire calorimeter) and temperature of the surroundings T_j (i.e. that of the calorimeter jacket) [2,9,10]. We can distinguish the following types of calorimeter: isothermal ($T_s = T_j =$ constant), including the solution ice or Bunsen calorimeters; adiabatic ($T_s = T_j \neq$ constant), suitable for measuring heats of reaction and heat capacities of relatively slow processes including dissolution; heat flow calorimeter, isodiathermal ($T_s - T_j =$ constant), useful for the direct determination of heat capacities and heats of transformation; or isoperibolic ($T_s - T_j \rightarrow 0$, $T_j \approx$ constant and T_s being measured). It follows that the quantities to be determined in almost all calorimetric experiments are changes in temperature, based on a knowledge of exactly what amount of substance is taking part in the reaction (assuming a particular reaction to occur). Only compensation calorimetry uses temperature differences exclusively for regulation, in order to maintain the samples in the preselected temperature programme (e.g. DSC).

The practical determination of reaction heats, heat capacities and all other thermal data begins with the selection of a suitable method. The most accurate way of determining heats is direct measurement of the heat effect of the actual reaction taking place in a calorimeter. The combustion bomb remains the standard apparatus for determining heats of formation of, for example, oxides. However, it requires skillful handling and careful analysis. Direct calorimetric determination of effects associated with mixing of liquids, particularly molten alloys, using conventional Calvet heat-flow or adiabatic calorimeters, has become a tradition. Solution calorimetry requires more time than direct calorimetry but has wider applicability. Thus, it is used for investigating heat effects associated with the 'freezing' of nonequilibrium structures and of other delayed transformations and is suitable, for example, for alloys as it allows treatment of alloys before dissolution. Since such heat effects are generally small their measurement requires the greatest accuracy and selection of a method which decreases errors. An example is where a solvent is selected in which the component studied has a low heat of solution; water, acids, liquid metals and/or oxide fluxes are among those in common use. Heat capacities can be derived from heat-content measure-

ments obtained by the popular drop-in isoperibolic calorimetry. Here it is necessary to prevent processes other than those to be measured, such as oxidation, decomposition or order–disorder transformations (including glass formation). In metallurgy, a popular method is the direct measurement of heating and/or cooling curves and also, occasionally, the measurement of heat fluxes from or into the sample [15]. (The corresponding differential method, called DTA [2], is the most frequent one in the thermochemical laboratory and will be dealt with in a separate paragraph.)

All the above-mentioned methods, however, have instrumental drawbacks and can only be used for the determination of phase diagrams together with direct observations of the structural state of the sample (by, for example, X-ray diffraction analysis, microscopy, etc.). This is, of course, the normal procedure for determining a phase diagram without analyzing it in more detail. Some specialized measurements, however, are worth mentioning. EMF measurements can be subdivided into three categories [13]: using galvanic cells with liquid electrolytes [16], with solid electrolytes [5] and with point electrodes [17]. The last, not so well known, has the advantage of quick investigation, as shown, for example, for ΔG measurements of Cu–Ca alloys [17]. Here CaF_2 pellets are employed as a solid electrolyte in planar contact with a layer of Ni/NiO electrode and having on its other side a two-point contact from Fe and Cu. The Fe point, on additional application of electric current, provides polarization of CaF_2 so that the metallic Ca is precipitated at higher temperatures. This can react with the Cu point, forming in this way alloys which are ready for direct measurement of ΔG. Another well-known technique is the determination of partial vapor pressures of a component above a solid sample, using fairly sensitive measurements (e.g. using TG) of larger amounts of the sample heated near the boiling points at preregulated pressures [16]. The effusion–Knudsen method [5] requires two separate measurements, the partial vapor pressure of a selected component in the alloy and that of the pure component at the same pressure. Very sensitive pressure detection is described, for example, in ref. 18. Using mass spectrometry, the ratio of the ion currents I_A and I_B (proportional to the partial vapor pressures p_A and p_B of components A and B) with the alloy atomic fractions x_A and x_B makes possible the calculation of the change of excess Gibbs energy ΔG^{EX} during a single measurement [19]

$$\mathrm{d}\,\Delta G^{EX}/\mathrm{d}x_A = \ln(I_B x_A / I_A x_B) RT + \text{const.} \qquad (1)$$

Another modification of the Knudsen method is the application of radioactive isotope tracers [20] and/or electron microprobe analysis [21]. In the dew-point method the equilibrium concentration can be continuously determined using, for example, electric conductivity measurements [22].

Equilibrium phase diagrams cannot, however, give any information about the reaction which transforms one phase to another, nor about the composition or structure of phases occurring under conditions other than those

which make equilibration possible. Under conditions of equilibrium of phases, when the chemical potential of the liquid phase μ_L^i (for each component i) is equal to that of the solid phase μ_S^i, the stable coexistence of both phases occurs. For a mathematical description, it is important how chemical potentials are expressed, i.e. to find a suitable strategy of phase diagram calculations. This is reviewed, for example, in refs. 23 to 26 and is applied to the computer generation of phase diagrams in refs. 27 and 28. The advantages of phase diagram construction using computers is documented by numerous specialised articles. Here, only a few dealing with heterogeneous equilibria are mentioned, for example describing data on liquidus curves in ternary systems [29], phase relations of multi-component systems in the subsolidus region [30], binary phase diagrams of compounds which do not form solid solutions [31], models of oxide melts [32], algorithmization of classical graphical treatment stressing phase coexistence at the invariant points [33], association models and glass formation in alloys [34] and prediction of eutectics and phase separation in the glass-forming region [35]. Here belongs the problem of how to express the non-ideality of solutions, as illustrated in Table 2 [36]. For a real system the system temperature deviates from that at equilibrium, and so the equality of chemical potentials is violated, producing in this way a driving force for the phase transformation. A measure of this force is the chemical potential difference $\Delta\mu_i = \mu_L^i - \mu_S^i$, i.e. for all $\Delta\mu_i < 0$ the solid phase melts and for all $\Delta\mu_i > 0$ the liquid phase solidifies [37]. In other words, this means that the new phase can be formed only under the nonequilibrium conditions of a definite driving force, and that at absolute equilibrium no new phase can originate. There thus arises a question of how to interpret experimentally-determined phase diagrams, which do not fully comply with equilibrium ones, their divergence being dependent on the proximity of the actual and the thermodynamically required conditions applied. Equilibration can be achieved under conditions of extremely slow cooling, (see Table 1) for which we must appreciate the change of thermodynamic state with time of such a non-isothermal experiment and the associated effect on the kinetics of phase transformation. The faster the phase transformation proceeds, the quicker is the system response to the introduced deviation from equilibrium, enabling a closer approach to conditions of equilibrium. On the other hand, there are cases where slowness of phase transformation can considerably affect equilibration. In an undercooled liquid the metastable phases can be frozen and if the viscosity increases rapidly with decreasing temperature the vitreous state can freeze in, resulting in an unstable solid state called a glass [2,36–39].

From the above analysis it follows that studying the time dependence of phase conversion is useful for a better understanding of transformation kinetics. At the same time the actual phase boundary between the two states investigated may be located [2,40–42]. It also makes possible determination

TABLE 2

Solid–liquid equilibria for a binary system of components A + B

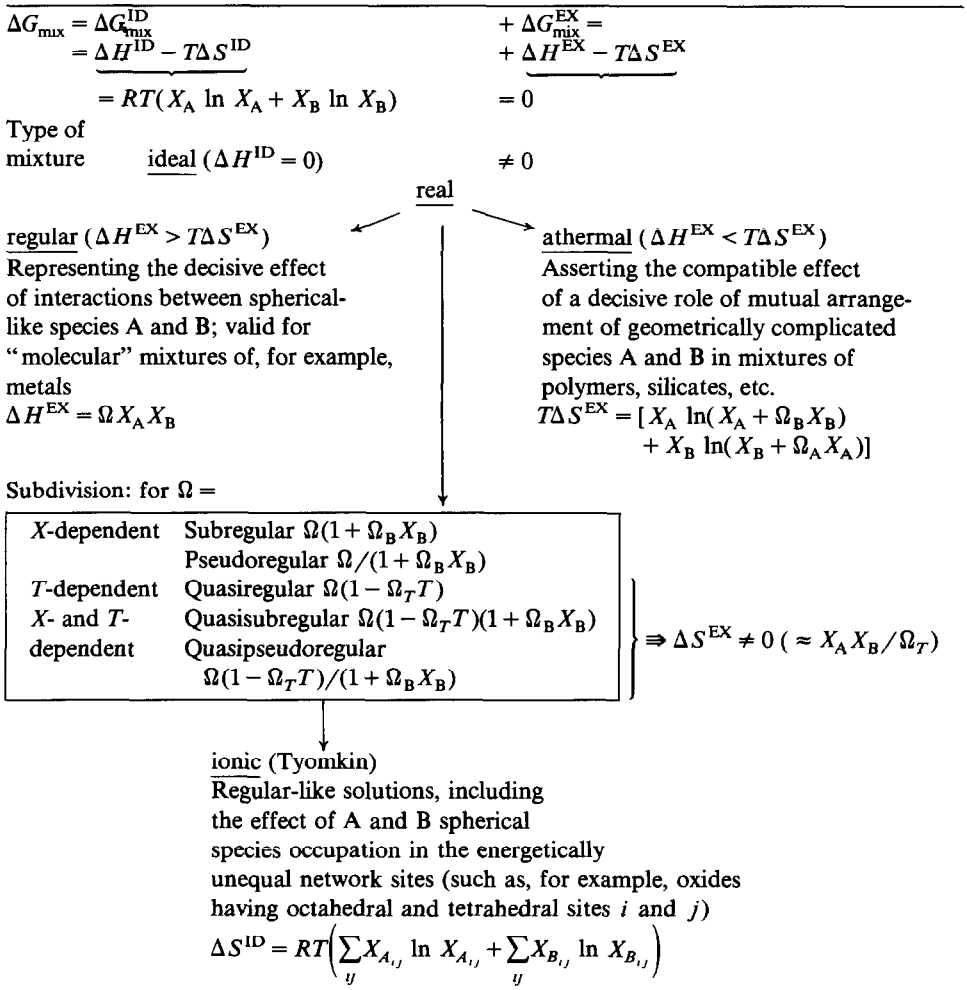

ID and EX indicate the ideal and excess values of the Gibbs energy G, the enthalpy H and the entropy S; Ω is the interaction parameter.

of the so-called T–T–T diagram (time–temperature–transformation). The T–T–T point is a certain time at which the degree of conversion comes into a definite value at a given temperature [2]. The T–T–T diagrams are of use for delimiting the minimum cooling rate under which a material can be vitrified [43,44] and are well known in metallurgy for specifying the formation of a given phase [40,42]. Metallurgists also first noticed the consequences of nonequilibrium solidification, i.e. phenomena called "coring" and "surrounding", which occur in the vicinity of invariant points. In the first case, the melt undergoing solidification cannot follow the solidus

equilibrium curve owing to insufficient mass transport to the phase interface [2,40]. The result is grains whose centres are closer to equilibrium composition than their outer part. In the second case, the originally precipitated phase starts to react with remaining melt on reaching the peritectic temperature, and forms a new peritectic phase. The atoms of one component must diffuse out from the melt to the phase interface. The thicker the layer is, the slower the diffusion proceeds, particularly if the atoms of the second component must diffuse in the opposite direction. This inevitably leads to nonequilibrium conditions of solidification and the creation of a phase which is increasingly less at equilibrium. Supplementary elimination of such nonequilibrium concentration gradients is usually accomplished by thermal treatment, in order to allow atoms to reoccupy their equilibrium positions. Similar phenomena are often met when studying single crystals grown from foreign melts whose concentration gradient is dependent on the concentration change in the matrix melt. Again, this can be removed by a specific treatment or by modification of the preparative conditions (e.g. melt circulation).

Some modern technologies (see Table 1) are intentionally based on such phenomena in order to create nonequilibrium phases of specific properties. Some examples are where new materials having modified physicochemical properties are prepared, which exhibit better magnetic, optical or mechanical properties, superconductivity, corrosion resistivity, catalytic activity, etc. [45–48]. A specific field covers materials prepared by ultrarapid cooling, which introduces some as yet unsolved problems into the fields of the chemistry and physics of solids [49,50]. By quenching the melts of alloys a great variety of metallic glasses have been obtained [51], the characteristic rate of cooling being about 10^6 K s^{-1} [52–57]. Relatively low melting temperatures and good electric conductivity (eddy current heating) without a specific need of high purity favor this technology. Typical compositions are about 80% metal (transition metal, noble metal or rare earth) and about 20% metalloids or other elements from Group IV or V of the Periodic Table. The best glass formation takes place in the vicinity of deep eutectic points. Another combination of two different metals, such as Cu–Ti, Nb–Ni, etc., has also been reported to form a glass near a eutectic point [52,53]. Such metallic glasses are very firm and hard but exhibit plastic deformation. Their structure is relatively simple compared with the other glasses (oxides). They have no grain interfaces and do not have many faults, which are unavoidable with ordered structures. In particular, they are very good magnetic materials having high permeability, low coercivity and low magnetic losses. Whilst studying the rapid solidification of Al–Mn alloys structures having a 5-fold rotational symmetry were identified [58–60] and named quasicrystals. Although the icosahedral structuring of Al atoms around the central Mn represents only a 1% change in their network compared with the original f.c.c. structure, the structural units having a 5-fold rotational symmetry

cannot form ordered crystalline materials displaying translational symmetry. Some theoretical studies have revealed that the undercooled melt has an icosahedral local structure. Below the equilibrium temperature there exists a correlation between the orientation of these icosahedrals which increases with decreasing temperature [61,62], possibly stimulating the formation of a glassy state. Similar processes proceeding far from equilibrium are detected by technologies which modify the surfaces of materials (mainly metals and semiconductors) using high-energy beams such as electron guns or, recently, lasers (with a density of about 1 J cm^{-2}). This enables us to obtain new controlled-surface structures having a very small size and precise localization, which is difficult to obtain by ordinary procedures. For example, it makes it possible to implant elements in alloy surfaces in concentrations and structures which are impossible to obtain under normal conditions of slow cooling, such as those for Si–Ge [63] or for the modification of thin layers of Si [64,65]. The rates of such ultrarapid cooling are estimated to be as great as 10^{11} K s^{-1}, yielding very limited heat transfer. This causes melt solidification into supersaturated solutions, quasicrystalline and/or noncrystalline phases because atoms cannot reach the near-equilibrium state with translational symmetry. Laser modification of surfaces also affects the distribution of defects, vacancies, dislocations, etc. A survey of methods and experimental evidence on certain materials is given in ref. 66 and of the use of the electron gun in ref. 67. Similar effects are achieved by applying very high dynamic pressures (10^6 bar) with resulting cooling rates of 10^9 K s^{-1} and pressure changes of 10^{12} bar s^{-1}. These are suitable for the preparation of metastable superconductors, magnetics, composites, etc. Besides the highly nonequilibrium processes encountered during rapid changes in external conditions [49] the metastable states can be obtained even at relatively slow cooling rates of $10–10^2$ K s^{-1} when studying very viscous materials (such as chalcogenides, oxides [70] and, particularly, silicates, e.g. the thoroughly investigated glass $Li_2O–SiO_2$ [68,69]).

Processes which are normally expected to produce equilibrated materials during single crystal growth may also form metastable phases different from those shown in the phase diagram. This is caused by the possibility of melt undercooling, as, for example, in the Co–Si system [70], where at slow rates of growth (at 1200 °C and 12.5 wt.% Si) the equilibrium eutectic Co + Co_3Si is formed. If nucleation is suppressed the metastable Co + Co_2Si can be found. Similarly, instead of equilibrium CdSb the metastable Cd_3Sb_2 can be grown (which requires cooling rates far below 10 K s^{-1}). Although these processes proceed near equilibrium, the properties of single crystals (texture, density of dislocations, impurity, lammeling, etc.) are very sensitive to small changes in the experimental conditions which determine the reaction (e.g. temperature fluctuation, concentration gradients at interfaces, liquid hydrodynamics, stability of external forces, etc.). It becomes important to find a correlation between the changes of given material properties as a response to

nonstability of experimental conditions of growth and/or to intentionally introduced alterations required to reach full experimental control.

II. FACTORS AFFECTING THE EXPERIMENTALLY RESOLVED SHAPE OF PHASE BOUNDARIES AND METHODS OF THEIR DETERMINATION

II.1. Experimental arrangements and the sample

While determining phase boundaries one encounters experimental factors of three different types [2,71]: (A) Arising from the nature of the material under study as associated with physico-chemical processes of sample preparation from raw materials; (B) affected by the experimental set-up; and (C) dependent on the kinetics of phase transformation. Group (A) can be further divided according to factors associated with sample processing because the given composition can be made using different preparative methods: (i) mechanically, i.e. by suitable homogenization of starting components (e.g. milling, grinding, mixing, etc.); (ii) chemically, i.e. by coprecipitation, freeze-drying or sol–gel reactions from a suitable aqueous or nonaqueous solution; and (iii) physically, i.e. by melting a mixture of starting components followed by solidification and mechanical treatment of the resulting solid.

A required tempered state for a given working temperature can be reached either "directly" (i.e. by time-consuming high-temperature firing) or "indirectly" on prereacted samples, by the action of increased pressure or of a dissolving substance. For slowly reacting systems, for example silicates, the attainment of a completely reacted state is difficult within real experimental times, and so it becomes more convenient to include the reaction kinetics directly in the real phase diagram than to seek increased reactivity (for example by firing the sample at higher temperatures than those required followed by annealing at a temperature lower than required). Special attention is required by such systems which interact with the surrounding atmosphere, i.e. which contain a volatilizable component of a certain partial pressure, such as oxygen in oxides, sulfur and arsenic in chalcogenides, etc. In such cases we perform temperature treatments as follows.

(a) At constant atmospheric pressure, leaving the sample free in its holder either in a static atmosphere inside the furnace or in a dynamic atmosphere of flowing air or another inert gas. In both cases hydrodynamic conditions play a decisive role in the transfer of volatilized components which are mainly localized in a gaseous envelope around the sample. A static atmosphere often leads to an increase in the local value of the partial pressure at the sample surface or between the grains of powder or polycrystalline sample.

(b) At constant partial pressure of the given component (e.g. O_2 for

oxides). This is ensured by means of a static reservoir of sufficient size at a given pressure (and often having pressure control), having the disadvantages of all static methods, or a stream of gas with a preset value of the partial pressure given by a suitable mixture of two mutually reacting gases, e.g. for O_2 by H_2/H_2O or CO/CO_2 or for S_2 by H_2/H_2S, etc.; a dynamic atmosphere saturated with the volatilized component at a temperature lower than that required for thermal treatment, e.g. for H_2O this involves bubbling the carrier gas through water or passing it over suitable hydrates, and for metallic As it involves connecting the reaction chamber with tempered As, etc.

(c) Isoactive firing of samples at constant volume, where for a given temperature the corresponding balance is carried out between the volatilized component of the solid and its surroundings. Here belong all experiments carried out in ampoules.

Group (A) also includes factors affecting the selection and control of the initial state of the sample [3,71], i.e. chemical and physical properties resulting from the material processing, such as composition compactness and homogeneity, impurity, sample diffusivity and viscosity and other internal dispositions, e.g. ability to form prenucleus sites as a result of prolonged tempering or creation of mechanical tensions and/or other internal forces.

Besides the interfering phenomena described above, group (B) includes all factors connected with the choice, experimental set-up and control of experimental measurements [3,71], i.e. (i) the effect of external forces during measurement (such as temperature, pressure, partial pressure, electromagnetic, hydrostatic, gravitational and other force fields) and particularly their changes (such as heating and cooling rates, change of atmosphere composition or convection instability, transformation of hydrodynamic conditions and resulting flows (cf. (ii) below), and (ii) the effect of sample geometry and of the measurement set-up (which includes factors affecting the generation and absorption of heat, the internal and external flow of heat and mass, the extent of volatile component generation and recombination and the interaction of interfaces and surfaces, which are all effective between the sample particles and between the sample and its holder and measuring devices.

Group (C) deals with the entire course of the phase transformation which determines the resulting structure and property of newly formed phases. Its understanding and detailed theoretical analysis is decisive for the prediction of experimental processes and is discussed in sections III–V below. In general, we can distinguish two basic stages of the process. These are the initial stage of new phase nucleation and the consequent growth at the phase interface (controlled either by boundary chemical reaction or by diffusion of reacting components to or from the interface). The total reaction outgrowth can be reversely affected by the experimental set-up as discussed above.

II.2. Thermometric measurements

Temperature measurement of the sample is one of the basic aspects of phase boundary determination when studying phase diagrams. Sample temperature is frequently determined using a mean value of the so-called centered temperature, which is valid under an assumption that the temperature measured in one part of the sample is sufficiently representative of that of other parts. The temperature depends on the size of the sample and any temperature gradients, as well as on good heat conductivity of the

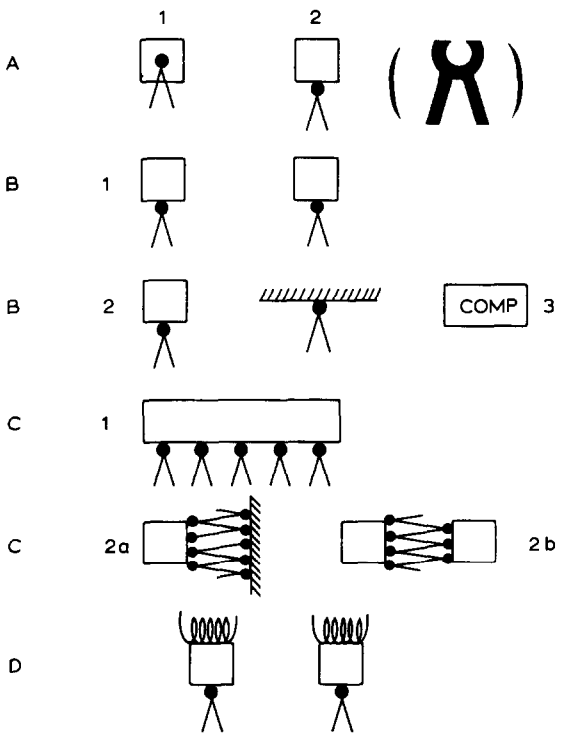

Fig. 1. Methods of temperature measurement with respect to sensor positioning. A, Direct, single (e.g. heating or cooling curve determination): 1, sensor inside the sample; 2, sensor in contact with sample surface (in the limit "sample inside the sensor"). B, Direct, twin (e.g. DTA): 1, two geometrically similar specimens (samples versus reference); 2, sample versus standard conditions; 3, direct single measurement where the reference is simulated by computer. C, Multiple, gradient (e.g. Calvet-type microcalorimetry): 1, Several sensors placed along the sample in the furnace temperature gradient; 2, thermopile (to ensure heat transfer taking place solely by conduction along the multiple thermocouple leads), (a) between the sample and the place of standard conditions, (b) between the sample and the reference. D, Compensation, nongradient (e.g. DSC): 1, microheater generation of heat to maintain both specimens at a preselected temperature (detected using method A). Other selections of relations between the compensation and spontaneous heat fluxes to match given calorimetric requirements are possible, e.g. measurement of temperature response (through behaviour of sample surroundings (similarly to B2 and C2a).

sample (or at least of the sample holder) to ensure good averaging of temperature along the sample surface. The type of temperature measurement is determined by the experimental set-up, particularly by the type of measuring head, and can be classified as direct, undirect, compensating, etc. (as illustrated in Fig. 1). Single or multiple sensors may be used.

No less important is the positioning of the sample with respect to the source or sink of external heat. The sample can be stationary or movable along or across the furnace. The furnace can exhibit homogeneous or gradient temperature distribution with constant or programmable temperature (as shown schematically in Fig. 2). The sample itself can be large (suitable for determining integral changes of, for example, enthalpy with possible elimination of temperature gradients by suitable melt stirring) or small (convenient for minimized temperature gradients in solids but with increased sensitivity surface phenomena which are usually negligible in large samples).

Factors arising from a real set-up of experiment which are often neglected are the following.

(a) A consequence of unequal heat absorption by the sample, sample holder and inside of furnace. Temperature gradients a priori measured in an empty furnace do not usually agree with the real gradients exhibited by the actual set-up when the sample with its holder is inserted into the furnace. For example, the sample holder can behave as a radiation shield (noble metals) or the sample can be transparent to infraheating (calomel). These considerably alter the original heat balance; in the first case a lower temperature and in the second case a higher temperature is measured than that corresponding to the actual temperature of the sample.

(b) A result of horizontal or vertical convection in a liquid sample caused by the following [70,72–88].

(i) Elevation of melt particles owing to a density difference which is a result of an inverse temperature gradient (against gravitation) or caused by thermally induced diffusion, by the temperature dependence of a chemical equilibrium or by concentration or dissolution, etc. This is the case most often found in the laboratory.

(ii) Liquid flow originating from a surface tension gradient along the free surface as a result of temperature or concentration inhomogenity (i.e. Marangoni flow) and/or different curvature. This effect is weak under normal conditions but becomes more important in gravitationless experiments with a free surface carried out in space or during the melt spinning technique for preparing metallic glasses in the form of thin ribbons.

(iii) Convection caused by the motion of a solidification front as a result of a difference in the specific volumes of liquid and solid phases. Such a primary flow exists in practically all investigated systems.

(iv) Flows caused by the effect of external force fields, such as centrifugal, electromagnetic, etc., acting on particles of the liquid phase.

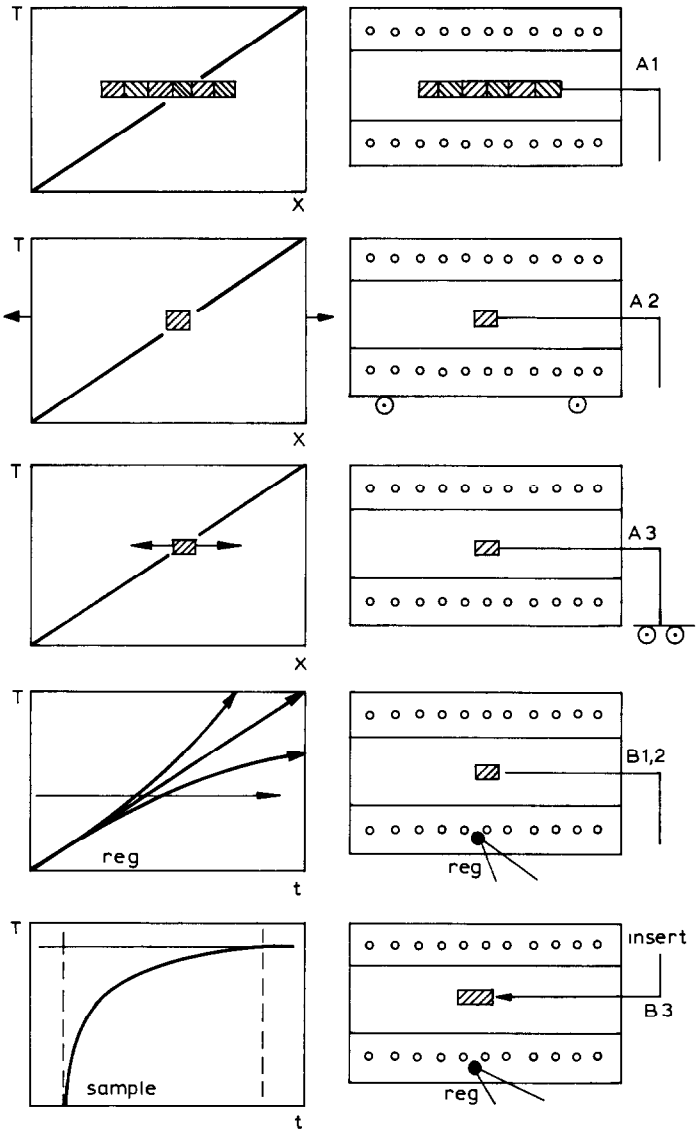

Fig. 2. Methods of sample temperature control using furnace design. A, Fixed temperature gradient: 1, multiple stationary samples placed along the furnace temperature gradient; 2, single stationary sample placed inside the movable furnace (used experimentally in e.g. zone melting); 3, single movable sample placed in the stationary furnace (e.g. Bridgemann method of single crystal growth). Controlled temperature gradient. In combination with A2, usually applied experimentally by means of computer. B, Programmed control of furnace temperature: 1, isothermal conditions; 2, non-isothermal conditions with hyperbolical, reciprocal or constant temperature increase (the latter method of constant heating is used in thermal analysis experiments); 3, spontaneous (non-regulated) heating, which is often applied in a reciprocal set-up where the sample is inserted into a pretempered furnace, e.g. drop calorimetry (it can also serve as DTA with exponential heating in the mode of computer-simulated reference).

It is worth noting that experimental evidence of the gradientless state of a large liquid sample is not proof of a gradientless arrangement, because the existence of a sample temperature gradient acting against the gravitational field results in intensive mixing of the melt in order to reduce the temperature differences. Occurrence of flows in melts causes the temperature fluctuation to increase, and thus also the transport properties of the liquid (which directly affect the stability, order and morphology of the phase interface [73,80,81,85]). Inclusion of convection into the theory of phase transformation is very difficult and has not as yet been satisfactorily achieved. Relevant studies [74–77,81–84,87,88] or numerical modelling for certain cases of crystal growth technology [78–80,86] give us a qualified picture of possible cases of convection, but entire utilization is very hard to deal with (usually owing to the limited capacity of computers and computing time). From the viewpoint of our more thermodynamically directed survey it has only a peripheral importance and so is excluded from further consideration.

II.3. Differential thermal analysis

DTA has become a very popular method in various fields of science because of its apparent simplicity—a series of thermal data may be collected in a single run. Not only may the process under study by measured but, at the same time, also the temperature deviation from the predetermined, usually linearly programmed, temperature increase. DTA simultaneously provides qualitative information about the position of the process along the temperature axis, quantitative data about the extent of reaction and finally kinetic data about the course of the reaction. The main problem of such quasistationary measurements is to decipher complex information hidden in a single DTA curve.

The DTA method belongs to indirect dynamic techniques in which a change of sample state is indicated as a temperature difference between the sample and a similar, inert reference under identical experimental conditions. Most commercial DTA instruments can be classified as double nonstationary calorimeters in which the thermal behaviour of the sample and that of the reference is compared. An advantage of this widely used method is the relatively easy verification of differences in thermal regimes of both specimens, and thus the determination of zero trace during a single measurement (commercial programmes ensuring conditions of constant heating and/or cooling). The relatively complicated relationship between the measured quantity ΔT and the desired quantity of enthalpy change ΔH has long been the major drawback in the quantitative and kinetic use of DTA. In accordance with refs. 89 and 90 and following the balance of thermal fluxes between specimens and their surroundings, the generalized equation of DTA was established [91–93]. Four essential requirements for

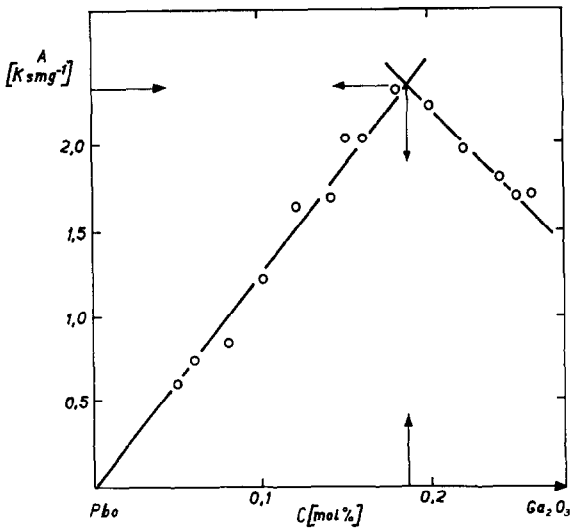

Fig. 3. Linear plot of amount of heat (in terms of peak areas A) against sample composition C experimentally determined using DTA.

correct DTA measurements follow from the analysis of the DTA equation: (i) attainment of a monotonous temperature increase; (ii) appropriate determination of characteristic points, such as the onset and tip of peaks, by extrapolation of base-line and peak branches; (iii) calibration of the temperature dependence of DTA instrument constants; and (iv) resolution of the s-shaped peak background necessary for refined kinetic evaluations.

It should be re-emphasized that during any DTA measurement the heating rate changes owing to the DTA deflection; at the point where completely controlled thermal conditions of the sample are achieved the entire DTA peak should disappear, thus demonstrating the contradiction between a nonstationary DTA measurement and the equilibrium-like conditions assumed for a phase transformation [94].

Nevertheless, a sequential investigation of samples of different compositions provides a series of traces which are useful for the exploratory determination of phase boundaries corresponding to certain peaks. Refinement of the position of invariant points can be done by plotting the area of successive peaks of fusion or solidification versus composition, to be fitted from both sides to a straight line. Their intercept [95] corresponds sufficiently well to eutectic or peritectic points; if calibrated they also reveal the enthalpy change associated with the extrapolated maximum peak area (see Fig. 3). It should be noted that, in the region between the solid and liquid phases, the less the solid phase melted per unit time the steeper the liquid phase curve. The DTA peaks of samples whose composition differs little from that of the eutectic are thus strongly concave, showing less sensitivity than the DTA peaks of compositions which differ greatly. Although the

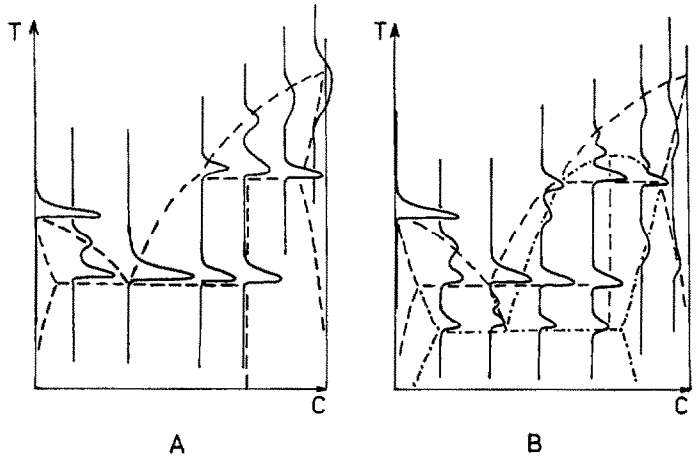

Fig. 4. Schematic picture of DTA responses as applied for determination of phase boundaries. A, Idealized DTA curves on passage through the phase boundaries (marked by dashed lines) obtained on heating a two component system containing solutions and exhibiting eutectic and peritectic points; B, as in A but assuming possible interference of changes taking place on extrapolated lines of metastable regions (indicated by dot-dash lines).

construction of a phase diagram purely on the basis of DTA curves looks simple (Fig. 4), it is rarely a case of very simply or ideally behaving systems. On monitoring the reactions of powders, especially in ceramic oxide systems [96], a complex pattern is obtained which exhibits a mixture of desired, equilibrium-like phenomena together with delayed or side-reactions. However, most misleading is the possible interference of metastable phases (see Fig. 4b), i.e. side-effects due to detection of extrapolated phase boundaries down into the lower-temperature metastable regions [97]. Similarly, it is difficult to determine precisely the peritectic regions, where the method of superposition of eutectic phase diagrams [71,94] seems to be useful (Fig. 5).

From the viewpoint of classification of phase transformations three basic types of DTA peak can be generally found.

(i) Peaks characterized by a single sharp apex typical of invariant melting or first order modification changes.

(ii) Peaks having rounded apices mostly representing the changes taking place in variant regions within a certain temperature interval. Besides the characteristic onset, we may also estimate the liquidus from the peak apex.

(iii) Traces characterized by two successive apices corresponding to passage through a two-phase region, i.e. eutectic or peritectic melting gives the first sharp peak (the onset representing the beginning of the fusion interval and the apex of the rounded second peak being the end point).

It is interesting that the characteristic profile of a DTA curve can, in fact, be derived from a derivative form of the ΔH versus T plot [2,94], which is particularly useful for describing the temperature behaviour of the unstable state of glasses [38,39]. Although mostly used for a hypothetical illustration,

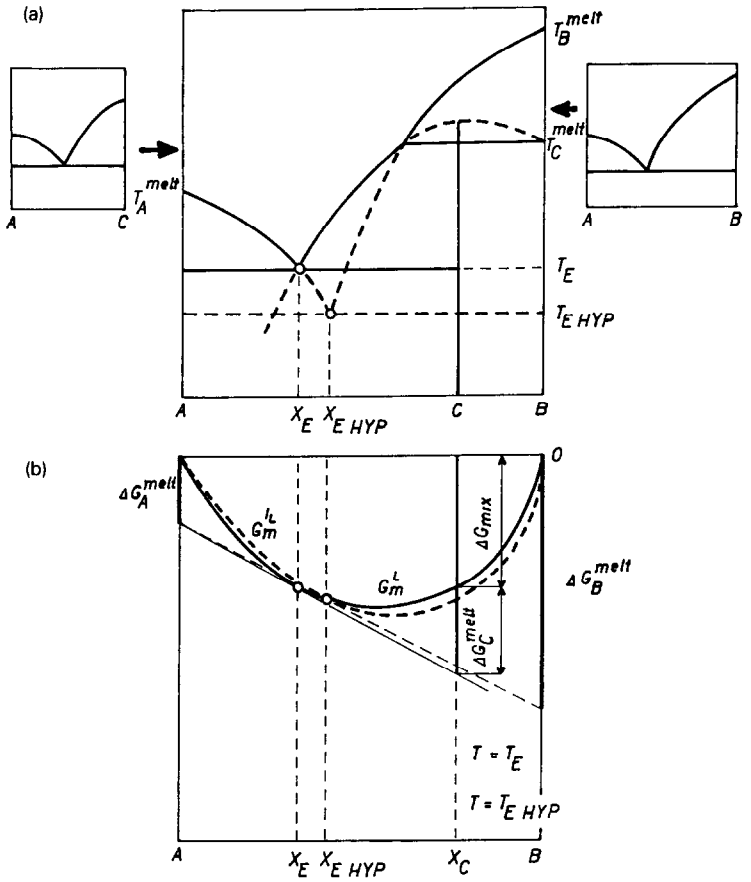

Fig. 5. (a) Schematic phase diagram of the system PbO (A) and Ga_2O_3 (B), experimentally investigated using the indirect dynamic technique of DTA (to observe formation and disappearance of phases) and the direct static method of X-ray diffraction (to indicate the existence of individual phases). Having no solid solution regions, the stable and metastable phase boundaries are shown by solid and dashed lines, respectively, showing hypothetical points (HYP) of a eutectic (E) and congruent melting (melt) of the phase $PbGa_2O_4$ (C). The phase diagram is a superposition of the two simple, eutectic-type phase diagrams A–C and A–B shown on each side. (b) Dependence of Gibbs molar energy on composition is presented using the classical common tangent method to illustrate both cases of stable and metastable phases coexistence at eutectic and hypoeutectic temperatures.

the actual ΔH vs. T plot can be derived using the lever rule from an equilibrium phase diagram (see Fig. 6), which can include the regions of metastability and glass formation. A further link can be introduced when assuming the third dimension: time (necessary to account for kinetic hindrance of processes occurring when crossing phase boundaries). The best representation is in the form of previously mentioned T–T–T diagrams [2,43,44] and is also included in Fig. 6 [94].

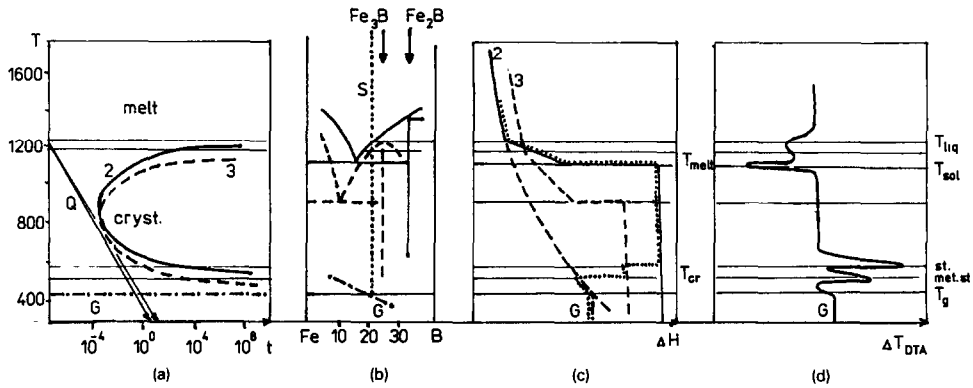

Fig. 6. A method of distinguishing possible processes taking place on heating (e.g. for a glass). (a) Binary phase diagram showing stable states (solid lines), metastable states (dashed lines) and glassy states (dot–dash lines). The vertical dotted line shows the composition in question. (b) Temperature dependence of enthalpy change (ΔH) derived from the preceding phase diagram by means of the lever rule. The possible course (dotted line) of consequent processes occurring on normal heating of the glassy state (prepared by melt quenching) goes through the metastable Fe_2B (T_{cr}^{mt}) and stable Fe_3B (T_{cr}^{st}) states into a liquid. The boundary lines express the limiting metastable and stable cases attainable under extreme conditions of ultrafast or ultraslow cooling and heating respectively. (c) The temperature derivative of (b) resembles the DTA recording. Each peak corresponds to an individual process shown by a step in the H vs. T plot. (d) Corresponding hypothetical T–T–T diagram (including time t for the extent of the reaction, 10^{-3}) with the stable and metastable areas again bounded by solid and dashed lines. The horizontal lines correspond to the glass transformation (T_g), crystallization (T_{cr}), peak (T_ξ) and melting (T_{melt}) temperatures, respectively. The arrows indicate the limiting rates of cooling (about 10^4 K s^{-1}) required not to touch the curve peak, if formation of a glass is desired.

III. NUCLEATION

Let us now look at the beginning of the phase transition, when the first clusters of the solid phase (that are able to grow independently) appear in the melt. This process is called nucleation. The nuclei of the new phase can be formed only from the supercooled melt, i.e. in a melt which is in a metastable state. The metastable state of the supercooled melt can differ from that of the melt by composition and structure at temperatures which are equal to or higher than the equilibrium temperature of the phase transition. Here complexes or clusters of a given symmetry, which can either facilitate or hinder the course of solidification are found [98,99]. On the other hand, spinodal decomposition of the melt can occur, when the melt decomposes to a number of non-mixing components. The influence of the composition of the metastable melt has not been included in the theoretical description of nucleation at present.

Essentially, we can distinguish two nucleation mechanisms: homogeneous and heterogeneous.

Homogeneous nucleation is the nucleation of the new phase in the bulk of the homogeneous melt, while heterogeneous nucleation is activated by impurities, defects and the surface of the melt and is connected with these inhomogeneities. Heterogeneous nucleation starts at a lower degree of supercooling in comparison with homogeneous nucleation, because the energy required for formation of the critical cluster is usually lower in this case. Homogeneous nucleation is more intense than heterogeneous nucleation at a higher degree of supercooling.

III.1. Homogeneous nucleation

In the initial stage of homogeneous nucleation clusters of several atoms or molecules form as a result of a fluctuation in the thermodynamic quantities. However, these small clusters are unstable because the influence of the surface energy predominates over the bulk energy. If the clusters reach the critical size, they are in a metastable equilibrium. The supercritical clusters become the nuclei of the crystal phase, and their further growth is advantageous from a thermodynamic point of view.

The nucleation rate $I(t)$ is the basic characteristic quantity in nucleation theory, which describes the number of supercritical clusters forming in unit volume per unit time. In fact, this quantity describes the kinetics of the initial formation of the new phase.

The nucleation rate will be constant at a constant temperature after a certain time. This value corresponds to the stationary nucleation rate I_S. The delay time (or the transient period, the induction time) is approximately the time required to reach the stationary nucleation rate, and it corresponds approximately to the moment when the first cluster appears. The delay time is extremely short and hardly detectable for phase transition from the vapor to the liquid phase. In condensed systems (glasses) the delay time is rather longer at 10^2–10^3 s [99–102]. In these systems it is important to include the delay time in order to correctly interpret the data for the phase transformation kinetics. The delay time must be relatively long in comparison with the cooling rate, in order to avoid experimentally detectable crystallization (e.g. for glasses) [103,104].

Fluctuation in formation of the clusters is connected with the work needed for their formation, and in the case of one component systems this is given for the liquid–solid phase transition by

$$\Delta G_n(T) = -n\ \Delta\mu(T) + A_n\sigma(T) \tag{2}$$

where $\Delta\mu$ is the supersaturation (i.e. the difference in the chemical potentials of the crystal and liquid phase at a given temperature), A_n is the surface of the n-sized cluster (that is, a cluster of n molecules or atoms) and σ designates the specific surface energy. In the case of binary systems it is necessary to consider the dependence on the concentration [105–108].

ΔG_n shows the maximum for

$$n^\star = \left(\frac{2\gamma\sigma}{3\Delta\mu} \right)^3 \tag{3}$$

where $n^\star$ designates the number of atoms (or molecules) in the critical nucleus and γ is the geometric factor depending on the cluster form.

$$\Delta G_{n^\star} = \frac{4\gamma^3\sigma^3}{27(\Delta\mu)^2} \tag{4}$$

It is apparent that the work needed for the formation of the critical cluster is sensitive to the value of the surface energy σ and to the supersaturation $\Delta\mu$. It is thus necessary to obtain exact values of these quantities in the analysis of nucleation. For example, the dependencies of σ on T or on the cluster size, etc. are considered [109,110].

Lothe and Pound [112] showed that the motion of the clusters must be computed for the nucleation in the vapor, which gives a further contribution to ΔG_n. This contribution is negligible in the condensed systems [104]. If we know the quantity $\Delta G_n(T)$, we can write a relation for the probability P_n of the occurrence of a cluster of a given size at temperature T

$$P_n \sim \exp\left(-\frac{\Delta G_n(T)}{k_B T} \right) \tag{5}$$

where k_B is the Boltzmann constant (P_n again strongly depends on σ and $\Delta\mu$).

It is assumed in the classical nucleation theories [112–115] that the dominant mechanism of the cluster growth is the gain or loss of single molecules on the cluster surface. Let $F_n(t)$ be the distribution function of the n-sized clusters at time t (i.e. the number of clusters of n atoms in unit volume). The evolution equation for the function $F_n(t)$ is given by [116]

$$\frac{\mathrm{d}F_n(t)}{\mathrm{d}t} = c_{n-1}F_{n-1}(t) + e_{n+1}F_{n+1}(t) - [c_n + e_n]F_n(t) = J_{n-1}(t) - J_n(t) \tag{6}$$

where the rate constants c_n and e_n are usually defined as the mean number of molecules passing per unit time from parent to newly forming phase and vice versa respectively at the surface of the n-sized cluster. The current $J_n = c_n F_n - e_{n+1}F_{n+1}$ gives the cluster formation rate for n-sized clusters. Equation 6 holds even for non-isothermal nucleation [117], but in this case the rate constants c_n and e_n are time dependent. If we interpret $c_n(t)$ as the probability of association of one atom on the n-sized cluster surface per unit time and $e_n(t)$ as the probability of the inverse process, we get a stochastic model of the nucleation. Equation 6 is the Fokker–Planck equation

[118–120]. The values of the rate constants in condensed systems were first published in ref. 121. The following relations were derived in ref. 122

$$c_n = A_n \rho_S \frac{k_B T}{h} \exp\left(- \frac{E_A}{k_B T} \right) \tag{7}$$

$$e_{n+1} = A_{n+1} \rho_S \frac{k_B T}{h} \exp\left(- \frac{E_A}{k_B T} \right) \exp\left(- \frac{|\Delta g_n|}{k_B T} \right) \tag{8}$$

$$\Delta g_n = \Delta G_{n+1} - \Delta G_n \tag{9}$$

where ρ_S is the surface density of atoms, h is the Planck constant and E_A is the activation energy for diffusion across the phase interface, which has a strong influence on the time evolution of the nucleation. It follows from the given relations that c_n and e_n again strongly depend on σ and $\Delta\mu$.

Let us look at the solution of eqn. 6. In the case of the stationary state, the currents $J_n(t) = K$ are independent of time and of the cluster size n, and the constant K is equal to the stationary nucleation rate I_S [37]

$$I_S = z c_{n^*} F_{n^*}^0 \tag{10}$$

where n^* denotes the critical cluster size and F_n^0 denotes the equilibrium cluster distribution function

$$F_n^0 = N \exp\left(- \frac{\Delta G_n}{k_B T} \right) \tag{11}$$

N is the number of single atoms in the system and z is so-called Zeldovich factor, given by

$$z = \left[\frac{1}{2\pi k_B T} \left(- \frac{\partial^2 \Delta G_n}{\partial n^2} \right)_{n=n^*} \right]^{\frac{1}{2}} \tag{12}$$

In the non-stationary regime at constant temperature, i.e. when the delay time is included, the nucleation rate depends on time. For this case, a set of approximate analytical solutions exist [123–128], which could be obtained from eqn. (6) or from the known Zeldovich–Frenkel equation [114,115], which is the limiting case of eqn. (6) for $n \gg 1$. Ref. 129 presents perhaps the sole exact calculation of the nucleation within the framework of renormalization group theory. On the other hand, solution of the non-stationary nucleation is possible by means of numerical computation. In ref. 130 there is a survey article about numerical computation of the nucleation within the framework of the Ising model [122,131–135]. It was shown on the basis of the numerical computations [134,136] that the best analytical treatment for non-stationary nucleation at constant temperature is given by Kashchiev [137]

$$I(t) = I_S \left[1 + 2 \sum_{k=1}^{\infty} (-1)^k \exp\left(- \frac{k^2 t}{\tau} \right) \right] \tag{13}$$

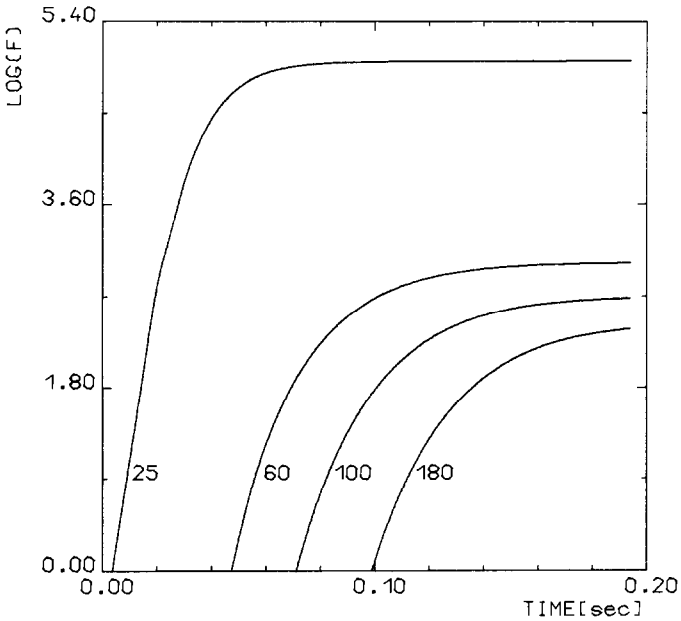

Fig. 7. Logarithm of the cluster distribution function as a function of time for cluster sizes of 25, 60, 100 and 180 molecules at $T = 822$ K in the case of nucleation from the $Li_2O \cdot 2SiO_2$ melt.

where

$$\tau = \frac{4}{\pi^3 z^2 c_{n^\star}} \tag{14}$$

In the general case, at non-constant temperature, analytical solution for the nucleation rate was not possible; only a quasistationary solution using certain restrictive assumptions was found [137]. On the basis of numerical computation of the kinetic equation, it is possible to obtain a set of quantities which characterizes the homogeneous nucleation process at constant and non-constant temperature [122,134] (see Figs. 7, 8 and 9).

Figure 7 shows the dependence of the logarithm of the cluster distribution function as a function of time for various cluster sizes in the case of nucleation from the $Li_2O \cdot 2SiO_2$ melt at $T = 822$ K [122]. It is evident from Fig. 7 that the time required to reach a stationary state depends on the cluster size.

Figure 8 shows the time dependence of the logarithm of the currents $J_n(t)$ at constant temperature. It can be shown from a theoretical analysis of the kinetic equation, eqn. (6), that the currents $J_n(t)$ have maxima at $n < n^\star$ [116]. This was confirmed by numerical computation. A stationary state was reached after a certain delay, which corresponds to the increasing function of the cluster size.

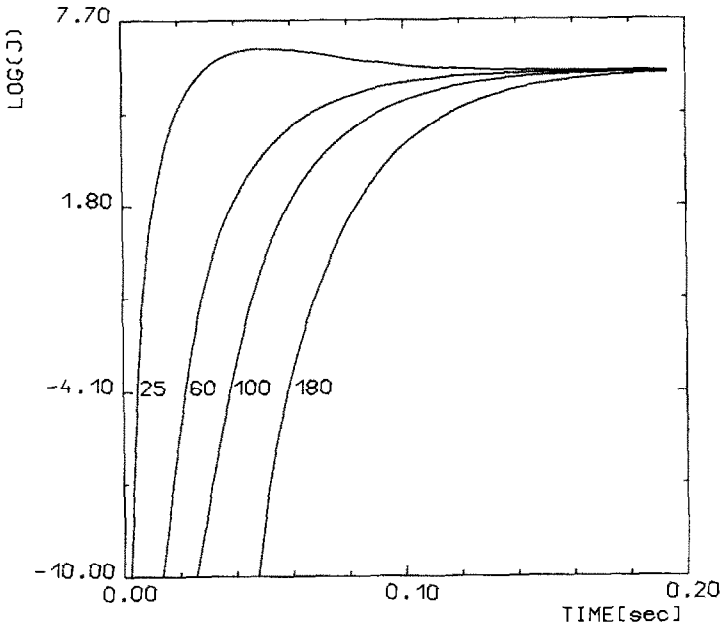

Fig. 8. Logarithm of the current J as a function of time for cluster sizes of 25, 60, 100 and 180 molecules at $T = 822$ K in the case of nucleation from the $Li_2O \cdot 2SiO_2$ melt.

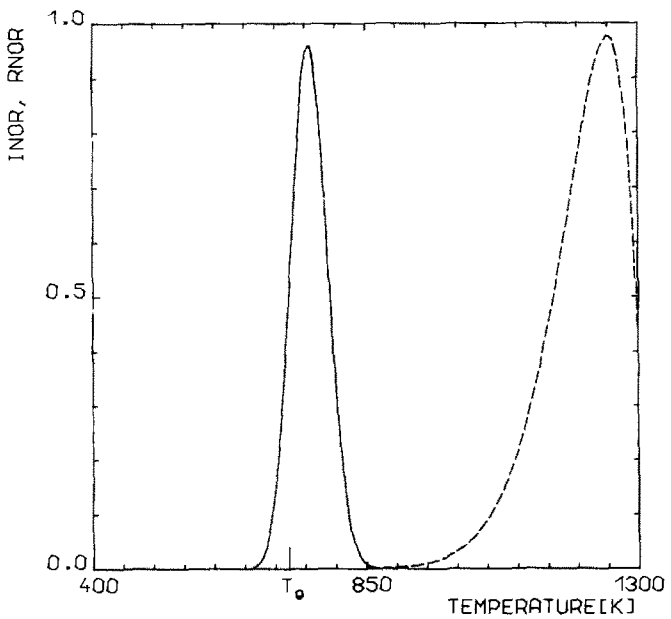

Fig. 9. Temperature dependence of the normalized nucleation rate $I_{NOR} = I_S/8.4 \times 10^7$ [m^3 s^{-1}] (solid line) and the normalized growth rate $R_{NOR} = R/5.8 \times 10^{-5}$ [m s^{-1}] (dashed line) for the $Li_2O \cdot 2SiO_2$ melt. T_g denotes the glass transition temperature.

It is evident from the temperature dependence of the stationary nucleation rate I_S and the growth rate R (see Fig. 9) for the $Li_2O \cdot 2SiO_2$ model melt, that the nucleation rate and the growth rate have extremum values at various temperatures. Only in a certain temperature interval do the nucleation and the growth of nuclei occur simultaneously, i.e. the volume crystallization occurs relatively quickly. Only fast cooling, i.e. relatively rapid passage through this temperature interval, enables the preparation of the glasses (see the following section concerning T–T–T diagrams).

In the case of non-constant temperature, it was shown that the current J_n depends on the cooling rate (see ref. 134), and the rate of formation of the critical nuclei decreases with increasing cooling rate. It was also observed that the critical size of the nucleus depends on temperature, and decreases with increasing undercooling. The nucleation rate is influenced by cooling or heating, when the subcritical nucleus becomes supercritical (and vice versa), and this fact is called athermal nucleation. Numerical computation [138] (where this phenomenon is automatically included) shows that with oscillating temperatures the nucleation rate increases (in comparison with constant temperature). This effect was experimentally observed by the authors of ref. 139. A survey of homogeneous nucleation may be found in ref. 140.

III.2. T–T–T diagrams

So-called T–T–T (time–temperature–transformation) diagrams are introduced for determination of the dependence of time required for formation of a given volume fraction crystallized at a particular temperature (see, for example, ref. 141). T–T–T diagrams characterize bulk crystallization and involve the nucleation process and further growth.

The volume fraction crystallized $X(t)$ at time t is given by the Johnson–Mehl–Avrami–Jerofejev–Kolmogorov equation [35,42,88–101, 141–147]

$$X(t) = \frac{V(t)}{V_0} = 1 - \exp\left[- \int_0^t I(t') v(t - t') \, \mathrm{d}t' \right] \tag{15}$$

where V_0 is the volume of the parent phase, $V(t)$ is the volume of the crystal phase at time t, I is the nucleation rate and $v(t - t')$ is the volume of the growing crystallization centre at time t which was formed at time t'. It has been shown that the additivity concept (based on the assumption that the momentary value of the transformation rate ($\dot{X} = \mathrm{d}X/\mathrm{d}t$) depends only on X and T and not on the temperature history of the transformation process) is advantageous for solution of the real non-isothermal processes. Šesták [145,146] and DeBruijn et al. [147] showed that at constant heating rate ($\dot{T} \neq 0$), a mathematical solution of the differential nucleation-growth equation gives the same results as in the classical case under isothermal conditions [2,36,148].

The computation of the volume fraction crystallized X is much easier if it is possible to separate the dependence $\dot{X}$ on the temperature from the dependence on X, i.e. to have the basic kinetic equation in the form $\dot{X} = k(T)/B(X)$, where it is possible to derive the functions $k(T)$ and $B(X)$ from classical model ideas involving nucleation, crystal growth and diffusion. Analysis of the DSC and DTA experiments also depends on the form of this function. In the general case under non-isothermal conditions [149]

$$k(T)\,\mathrm{d}t = B(X)\,\mathrm{d}X = \mathrm{d}b(X) \tag{16}$$

and the solution of this equation at $\dot{T} = 0$ is $b(X) = k(T)t$ (where $b(X)$ denotes the basic function of $B(X)$). The time t_a required for reaching the defined transformation degree X_a is then given by $t_a(T) = b(X_a)/k(T)$.

In the case of the spherical nucleus form and at a constant growth rate R

$$v(t) = \tfrac{4}{3}\pi R^3 t^3 \tag{17}$$

In the case of multicomponent systems, the growth rate of the crystallization centre is limited by diffusion processes. In such a case $R \sim t^{1/2}$ and $v \sim t^{3/2}$ [37]. The same dependence of the volume of the growing crystallization centre is observed in the case where the growth of the nucleus is limited by heat transfer.

If the nucleation rate is stationary (i.e. if it is possible to neglect the delay time) and the growth rate of the crystallization centre is not limited either by heat transfer or by diffusion, the following equation holds in the initial stage of crystallization ($X \ll 1$)

$$X(t) = \frac{\pi}{3} I_S R^3 t^4 \tag{18}$$

This effect must be included in the computation of the volume fraction crystallized in such a case, where it is not possible to neglect the delay time for reaching stationary nucleation [150]. A more exact analysis of the volume crystallization is based on computation of the size-dependent cluster distribution function of the newly forming phase, which characterizes more accurately the state of the system [122,151,152]. Some results of the numerical computation are illustrated in Fig. 10 (see ref. 122).

Figure 10a shows the T–T–T diagram for various values of the crystallization fraction X and for various approximations of the supersaturation $\Delta\mu(T)$ as a function of the temperature. Figure 10b shows the T–T–T diagram for various values of the surface tension. Figure 10c shows the influence of the phase equilibrium temperature T_E on the volume crystallization. Figure 10d shows the influence of latent heat on the T–T–T diagram. Figure 10e shows the influence of the wetting angle ϑ on heterogeneous nucleation.

Within the framework of phenomenological field theory of the phase transformation based on the Landau–Lifschic form of the free energy, the

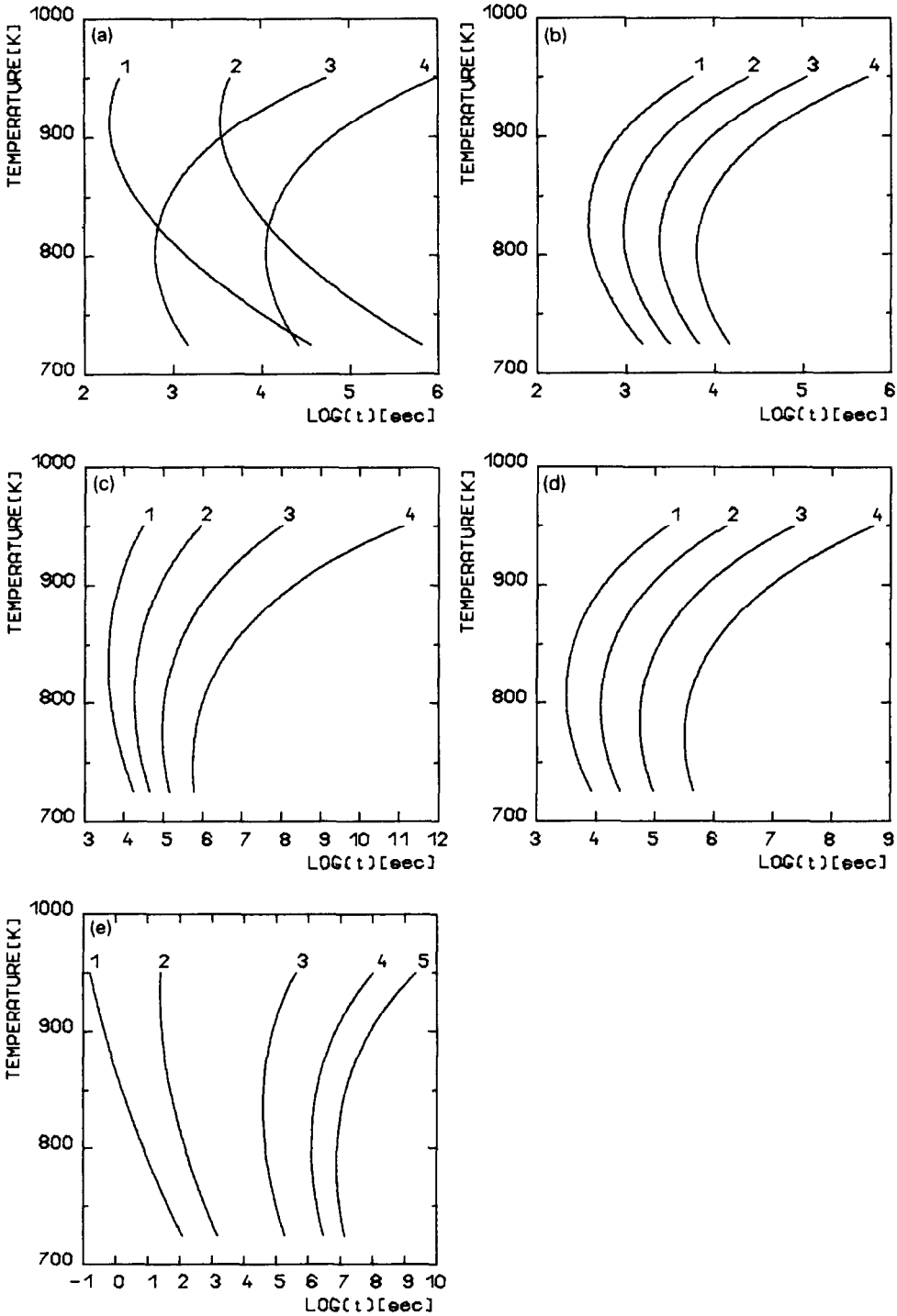
(a)
(b)
(c)
(d)
(e)
TEMPERATURE[K]
LOG(t)[sec]
1000
900
800
700
1
2
3
4
5

most successful description of the nucleation processes with further growth has until now been given in ref. 153. T–T–T diagrams can be used, for example, for the study of glass states. If we want to carry out analyses of glass state creation, it is necessary to define this glass state. Uhlman [154] proposed for the upper limit of the crystallization phase in the glass state the value $X_d = 10^{-6}$, which is lower than the experimentally observable value. It is possible to estimate from the T–T–T diagram the characteristic minimum cooling rate $\dot{T}_{min}$, which is sufficient for a melt to transfer to the glass state.

$$\dot{T}_{min} \approx (T_E - T_X)/t_X \tag{19}$$

where (T_X, t_X) is the point of the T–T–T diagram corresponding to the minimum time t_X needed for formation of the crystallization fraction X_d; T_E denotes the crystallization equilibrium temperature.

It is possible to get a more accurate estimation of the critical cooling rate from a construction of the continuous cooling curves, i.e. from T-C diagrams (cooling). This method was first used in refs. 109 and 155. The curves constructed for conditions of continuous cooling show that, in comparison with the T–T–T diagram, the same crystallization degree is reached at a relatively lower temperature and in longer times.

III.3. Heterogeneous nucleation

Heterogeneous nucleation is different from homogeneous nucleation in the size of the crystallization center on which the nucleus of the new phase can be formed (it is smaller in comparison with homogeneous nucleation) and in the work needed for critical nucleus formation (it is usually lower than in the case of homogeneous nucleation). The work needed for critical heterogeneous nucleus formation $\Delta G_{n^*}^{HET}$ for a spherical approximation of the surface of a crystal nucleus is given by [37]

$$\Delta G_{n^*}^{HET} = \Delta G_{n^*} \Psi(\vartheta) \tag{20}$$

Fig. 10. Influence of various parameters on T–T–T diagrams for the $Li_2O \cdot 2SiO_2$ melt. (a) T–T–T diagram for various values of the crystallization fraction X and for various approximations of the supersaturation $\Delta\mu$. Curves 1 and 2, $\Delta\mu = (\Delta h_E(T_E - T)/T_E)(T/T_E)$, $\sigma = 0.117$ (J m^{-2}); curves 3 and 4, $\Delta\mu = (\Delta h_E(T_E - T)/T_E)$, $\sigma = 0.160$ (J m^{-2}). $X = 10^{-6}$ for curves 1 and 3 and $X = 0.1$ for curves 2 and 4. (b) T–T–T diagram for various values of the surface tension σ. Curve 1, $\sigma = 0.148$; curve 2, $\sigma = 0.152$; curve 3, $\sigma = 0.156$; curve 4, $\sigma = 0.160$ (J m^{-2}). (c) T–T–T diagram for various values of the equilibrium temperature T_E. Curve 1, $T_E = 1400$ K; curve 2, $T_E = 1350$ K; curve 3, $T_E = 1300$ K; curve 4, $T_E = 1250$ K. (d) T–T–T diagram for various values of the latent heat Δh_E. Curve 1, $\Delta h_E = 10^{-19}$; curve 2, $\Delta h_E = 0.95 \times 10^{-19}$; curve 3, $\Delta h_E = 0.9 \times 10^{-19}$; curve 4, $\Delta h_E = 0.85 \times 10^{-19}$ (J molecule^{-1}). (e) T–T–T diagram for various wetting angles ϑ in the case of heterogeneous nucleation. Curve 1, $\vartheta = 45°$; curve 2, $\vartheta = 70°$; curve 3, $\vartheta = 100°$; curve 4, $\vartheta = 120°$; curve 5, $\vartheta = 140°$.

where

$$\Psi(\vartheta) = \tfrac{1}{4}(1 - \cos\vartheta)^2(2 + \cos\vartheta) \tag{21}$$

ϑ is the wetting angle between the newly forming crystal phase and the surface, where nucleation occurs. The work needed for critical nucleus formation decreases with decreasing wetting angle ϑ, and therefore nucleation is easier at these surfaces in comparison with homogeneous nucleation. In contrast to homogeneous nucleation heterogeneous nucleation occurs even at low degrees of undercooling. This is a result of the lower energy barrier for critical nucleus formation in the case of heterogeneous nucleation.

If the liquid contains a small amount of active admixtures, the nucleation rate of homogeneous nucleation is higher at a higher degree of supercooling than the nucleation rate of heterogeneous nucleation. The weaker temperature dependence of the stationary heterogeneous nucleation rate in comparison with that of homogeneous nucleation permits the experimental separation of the influence of homogeneous and heterogeneous nucleation [37].

III.4. Nucleation in binary systems

Analysis of nucleation in binary systems is complicated by the existence of a further parameter on which the nucleation process depends, namely the concentration C of one component in the system. The work needed for nucleus formation of the new phase in the parent phase, ΔG, depends not only on the temperature and on the number of atoms in the nucleus, but also on the concentration. This function ΔG has an extreme value at a saddle point (in the surface ΔG in the space (n,C)), which is defined by

$$\frac{\partial \Delta G}{\partial n} = 0 \tag{22}$$

$$\frac{\partial \Delta G}{\partial C} = 0 \tag{23}$$

The values of the concentration $C^\star$ and of the nucleus size $n^\star$ which are equivalent to the values of the critical nucleus in one-component systems correspond to this saddle point. It is therefore assumed in stationary nucleation theories that the growth of the new phase passes over this saddle point. These theories are given, for example, in refs. 156–166, where it is possible to find model relations for the function ΔG. The field theories, which are based on the Landau–Lifschic form for the free energy, deal with nucleation in binary systems and are given in refs. 167–170. It can be shown (see ref. 171) that, in the case of equilibrium of the critical nucleus in the system, the concentration corresponding to the conditions of eqns. 22 and 23 is identical with the concentration corresponding to the equilibrium phase diagram of a given binary melt (at low supercooling).

In binary systems, further growth of the nuclei is influenced by the concentration distribution as well as by the temperature distribution. This phenomenon was studied in the growth of a single nucleus of spherical shape, including diffusion in the surrounding neighborhood [172–175]. In these papers it was shown that the concentration of the nucleus changes with the nucleus radius, and for large radii it approaches the growth of the plane interface; the rate of the solidification changes with time. During the growth of these nuclei equilibrium conditions are assumed at the phase interface. The influence of supersaturation of the single components of binary systems on the mean concentration of the nuclei was also studied [176,177]. For a high level of supersaturation most of the nuclei shift from the saddle point (see refs. 178–182). The thermodynamic conditions for formation of the nuclei of the metastable phase from the undercooled melts were investigated. It was shown that a change in temperature changes the position of the saddle point, and that the composition of the critical nucleus depends on the supercooling (it may differ from the composition which corresponds to the equilibrium composition). Isoconcentration nucleation of the hypothetical ideal solution most probably occurs at temperatures $T = T_E/3$, where T_E is the equilibrium temperature of the solidification.

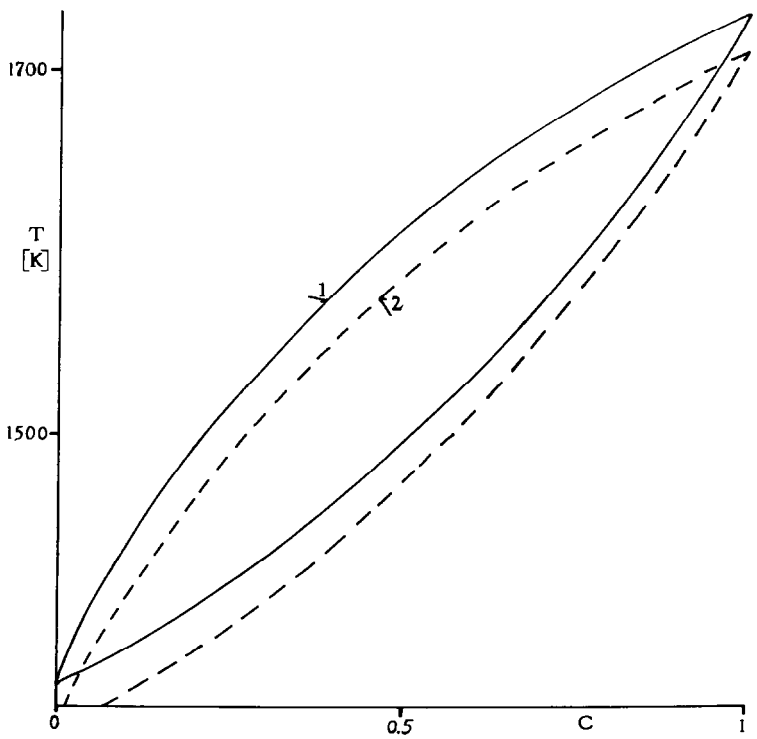

Fig. 11. Kinetic phase diagram of Cu–Ni alloy during the nucleation process. Average velocity of molecules $v_m = 10^{-3}$ m s^{-1}, cooling rate $\varphi = 0$ K s^{-1} (1), 10^8 K s^{-1} (2).

Binary nucleation is studied in the system where two partly non-mixing components exist in the liquid phase (see ref. 183). In such a system, nuclei of each non-mixing component can be formed. The case where the critical nuclei of both phases have the same value for the free energy of formation and then nucleate at the same frequency could occur.

Besides the above-mentioned dependences the influence of the cooling rate and of the external conditions on the nucleation of multicomponent systems were studied. Within the framework of the stochastic theory of nucleation (see ref. 184), the form of the phase diagrams was derived for the nucleation process of binary systems. These diagrams give the temperature at which the first critical nucleus of the solid phase is formed, and the critical nucleus composition as a function of melt composition and cooling rate. In the case of phase equilibrium, these diagrams approach the equilibrium phase diagrams (see ref. 171).

Figure 11 shows the phase diagram for Cu–Ni alloy. The influence of convection in the melt on the nucleation process was studied in ref. 184 (Fig. 12). The undercooling occurring on formation of the first critical nucleus decreases with increasing mean velocity of the molecules, and the concentration of the solid phase approaches the concentration which corresponds to

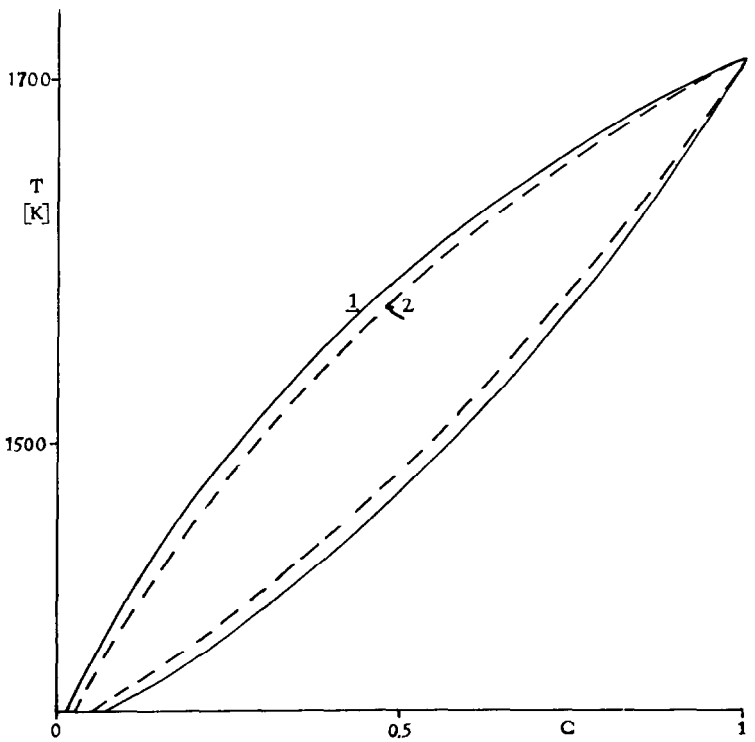

Fig. 12. Kinetic phase diagram of Cu–Ni alloy during the nucleation process. Cooling rate $\varphi = 10^8$ K s^{-1}, average velocity of molecules $v_m = 10^{-3}$ m s^{-1} (1), 10^{-5} m s^{-1} (2).

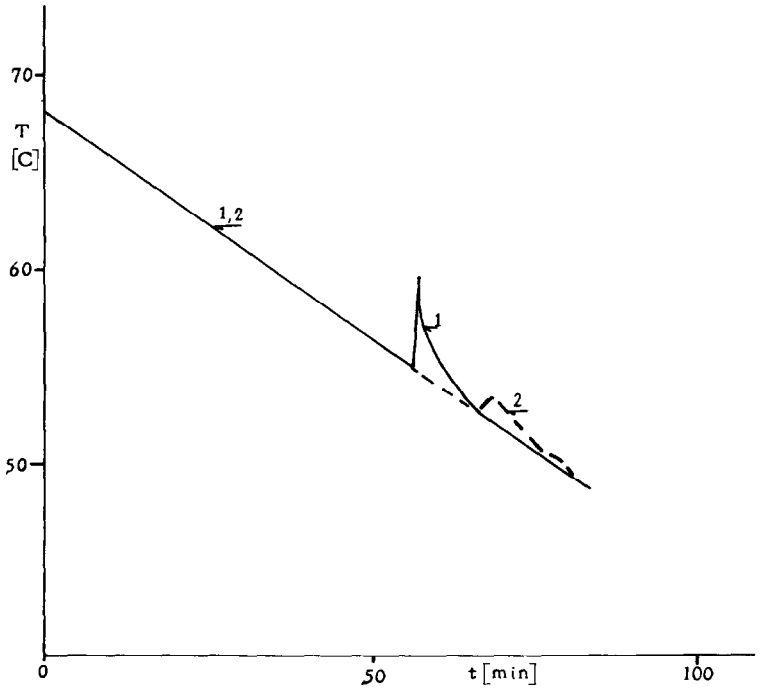

Fig. 13. Thermographic plots of the crystallization process. In diffusive heat transfer (2), nucleation starts at a higher supercooling of the solution than during convective transfer of heat (1).

equilibrium conditions. This fact was experimentally observed in ref. 185, where convection in the melt phase was altered because of a change in the viscosity of the melt from which the solid phase nucleated (see Fig. 13). It follows, from this analysis and from the model cases, that it is necessary to devote major attention to the influence of external conditions (cooling rate, convection, external field, etc.) on the nucleation process. This is especially so for conditions which occur in extremum conditions (fast cooling, high or zero gravity, etc.). At the same time, much attention must also be paid to the state of the supercooled liquid phase.

IV. GROWTH AT THE PHASE INTERFACE

Phase transformation occurring at the phase interface is, as far as we can tell, completely opposite to nucleation. In the case of homogeneous and heterogeneous nucleation, the new phase in the medium of the liquid phase is formed mainly in consequence of fluctuations. In growth at the phase interface, on the other hand, the new phase already exists in the system. This is why the phase transformation occurs via a different mechanism with a lower energy barrier. In practice this means that rather less undercooling is

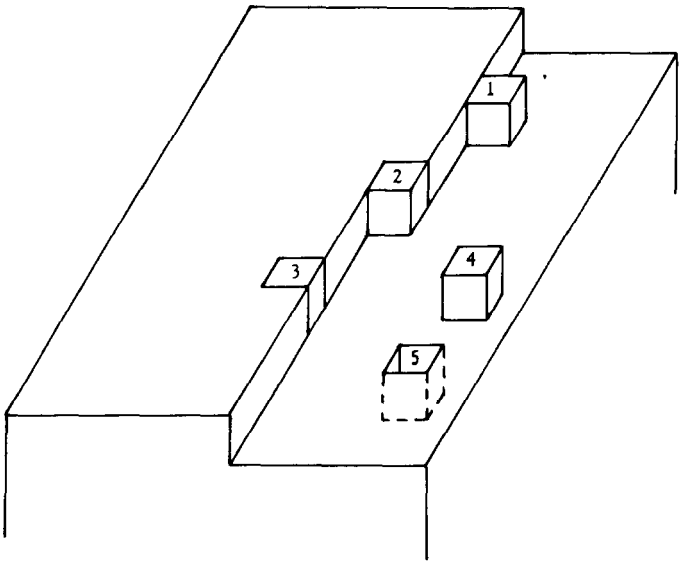

Fig. 14. Different positions of atom adsorptions during growth: 1, ledge ad-site; 2, kink; 3, ledge hole; 4, surface ad-site; 5, surface hole.

usually necessary for the growth of the new phase. However, this undercooling depends on the cooling rate and may be influenced.

The final growth process at the phase interface is influenced both by mass transport to the interface and by heat transport (by diffusion or convection), and also by the kinetics of the phase transformation itself, which may also change during the process and which is connected to the structure of the phase interface (see, for example, ref. 186).

The phase interface, which we comprehend as the region between the "perfect" solid phase and the "perfect" liquid phase, can be sharp (there is an immediate change from the solid to the liquid phase, i.e. changes in physical quantities occur over the distance of one lattice parameter) or diffuse (layers exist at the phase interface and it is not possible to say clearly if they belong to the solid or to the liquid phase; changes in physical quantities occur over the distance of several lattice parameters). A further possibility is that an absorption film (or quasiliquid layer) is formed on the surface of the solid phase, which usually has a higher concentration of dissolved substance in comparison with the liquid concentration [187].

In the case of the sharp phase interface we can divide the surface into two types: atomic smooth (without overhangs, steps or "kink sites") and atomic rough (where kink sites prevail (see Fig. 14)).

A theoretical description of the structure of the phase interface is dealt with in refs. 188–191. The stability of the transition layer in the stationary regime (when the growth rate $R = 0$) is given in refs. 192 and 193.

The quality of the phase interface depends partly on the quality of the liquid and solid phases (on the difference between the free energies), and partly on the temperature (on the degree of supercooling). Analysis of the behaviour of the thermodynamic quantities which characterize the phase interface is given in refs. 194–198 within the framework of the theory of discontinuity surfaces. In these references the basic thermodynamic equations which describe the conservation laws of mass, energy and impulse on the phase interface, which are connected with the flow of these quantities and with the surface curvature, were formulated. These equations may be used as the boundary conditions of the equation describing mass and energy transport in the bulk phases.

Large numbers of works [199–201] are devoted to the diffusion interface, but hitherto it seems possible to explain the known data of the kinetics of crystallization only on the basis of the sharp interface [187].

Burton, Cabrera and Frank [202] introduced the so-called "terrace–ledge–kink" model, and showed that under a certain critical temperature T^R (roughening temperature) the crystal surface is atomically smooth, whereas at temperatures $T > T^R$ the surface is atomically rough (the edge free energy vanishes). They used the exact Onsager solution [203,204] for the Ising model for spin $-1/2$ and obtained

$$\frac{k_B T^R}{\Phi} = 0.567 \tag{24}$$

for the square surface lattice, where Φ designates the binding energy. For the vapor–solid interface eqn. (24) gives T^R above the temperature of melting. This is not observed in the set of materials.

Jackson computed the change in Gibbs energy for the addition of molecules of the coexisting melt onto the plane surface, assuming a random molecule distribution in a mean field approximation, and he derived a widely used factor for the determination of the surface roughness [205]

$$\alpha_J = \frac{L}{k_B T} f_{hkl} \tag{25}$$

where L is the internal energy change per atom (often approximated by the latent heat) and the anisotropy factor f_{hkl} is the ratio of the number of lateral neighbors of an atom from the crystal surface and the bulk coordination number. This gives the rough interface for $\alpha < \alpha^R$ and the smooth interface for $\alpha > \alpha^R$, where α^R designates the critical α value for which Jackson obtained $\alpha^R = 2$ for the (001) vapor–crystal interface of the Kossel crystal (i.e. a simple cubic crystal with only nearest neighbor interactions). This approximation gives the rather higher T^R value in comparison with the result of eqn. (24). Jackson's α factor gives a good approximation to T^R for the melt–crystal transition, but the theoretical values for the vapor–crystal transition give a higher T^R value in comparison with experiment. If we

include surface relaxation in the computation of the surface roughness, i.e. if we assume that the binding energy of the solid phase near the surface is different from that in bulk, we obtain agreement with the experimental data even in this case [206].

Van Geijeren [207] and Knops [208] elucidated the character of the roughening transition. It was shown that the roughening transition has an infinite order, i.e. all derivatives of the free energy with respect to temperature are equal to zero at the transition point.

Wilcox [209] assumed that the surface is formed by a set of steps, and he showed that the number of steps increases with increasing temperature gradient, i.e. the surface becomes rough at sufficiently high temperature gradients.

If the crystallization motive power ($\Delta\mu$) is higher than a certain critical value, the surface becomes rough even below the roughening temperature T^R, and so-called kinetic roughening occurs [210].

The models of the dependences of growth rate on supercooling are summarized in ref. 75. The rough surface models (Jackson's model) are compared with the Monte-Carlo computation method. In this work the existence of kinetic roughening is also shown.

The problem of quasiliquid layer formation on the crystal surface during growth from the vapor has been investigated since about the forties. Stranski [211–213] considered that a necessary condition for quasiliquid layer formation is the total wetting of the crystal surface by the parent liquid. This condition was used later as the basis of a phenomenological study of the problem [214,215]. Numerical simulation of the molecular dynamics [216,217] confirmed the existence of quasiliquid layer formation on the crystal surface. Hitherto neither surface roughening nor the existence of the quasiliquid layer was experimentally observed [218]; there existed only indirect experimental data [219–227]. Experimental data concerning the existence of a quasiliquid layer on the crystal surface and the structure of this surface are not simultaneously available. Recent experiments support a difference between surface melting and roughening [218].

The vapor–liquid–crystal mechanism is the basic mechanism of needle crystal growth. The growth rate $R \sim (\Delta\mu)^2$, where $\Delta\mu$ is the difference between the chemical potentials of vapor and crystal phases. In typical cases, the energy of the crystal–melt interface is 5–10 times lower in comparison with the energy of the crystal–vapor interface. For this reason the nucleation rate of two-dimensional nuclei at the liquid–crystal interface is much higher than at the vapor–crystal interface.

Several mechanisms of phase transformation kinetics, based partly on phase interface quality and partly on the thermodynamic properties of the system, have been suggested.

Gilmer (see ref. 228) used the initial properties of the growth rate on the phase interface together with the following models: the Ising model, the

Monte-Carlo model and two-dimensional nucleation. In this analysis it was shown that growth rate oscillations, which disappear above the roughening temperature, can exist below the roughening temperature. In ref. 229 the connection between the phase interface dynamics and the interface structure was studied.

Layer growth is usually assumed to occur during growth at the atomically smooth surface (when steps are formed on the surface), which spreads at a certain lateral velocity. A step is defined as the boundary between one part of the smooth surface and a second part which is one layer thickness higher. Numerical computation has shown that growth on the surface occurs as long as attainable steps exist on the surface [230–232]. A number of models is used according to the origin of the step formation. Growth then follows the "current" of the steps along the surface [233].

Before lattice defects were recognized as a possible source of the steps, it was assumed that growth on the smooth interfaces could occur only by surface nucleation with the further growth of two dimensional nuclei (the height of a nucleus is equal to the thickness of a layer). Modern solid state technology, which enables us to obtain crystals without defects, provoked a new interest in growth by the heterogeneous nucleation mechanism. On the crystal surface, adsorption, diffusion, collisions between molecules (or atoms) and desorption exist. Clusters of the several molecules, which can decay, are formed, but growth is advantageous from a thermodynamic point of view if they reach a certain critical size. The formation of the critical nucleus is the key factor in all two-dimensional models (in a similar way to homogeneous nucleation). It is also possible to determine the work needed for critical nucleus formation and its size by a similar method to that in homogeneous (three-dimensional) nucleation [233–236]. The growth rate of the phase interface R is proportional to $\exp(-C/\Delta\mu)$. It is possible to divide surface nucleation theory according to the relative time scale of the nucleation rate and the lateral growth rate v_1 (the rate of spread of steps along the surface) into the following models [225].

(i) Mononucleus model ($v_1 = \infty$, i.e. the entire monatomic layer forms at the moment of formation of the first critical nucleus).

(ii) Polynucleus model ($v_1 = 0$, i.e. a sufficient amount of critical nuclei must be formed in order that layer formation may occur).

(iii) Birth and spread model ($v_1 = \text{constant} \neq 0$, i.e. growth follows nucleation and further lateral growth at a finite rate).

It can be shown that the height of the nucleus may not be mononuclear during surface nucleation, but depends on the surface energy at the phase interface and on the degree of supersaturation $\Delta\mu$ [237,238].

Two-dimensional nucleation in binary systems has been studied by various workers [239–242]. In these works the dependence of surface energy on concentration is considered, and the saddle point in the dependence on energy of formation of a two-dimensional nucleus as a function of size and

concentration is established. The growth rate of the phase interface is also determined. The influence of defects in the phase interface on surface tension and on growth is investigated in ref. 239.

Many crystal surfaces grow relatively quickly at a relatively low degree of supercooling, and this cannot be explained by the surface nucleation mechanism [234]. Frank et al. [202,243] suggested a spiral growth mechanism being a permanent source of the steps. The screw dislocations, which have the greatest influence on the growth kinetics at low degrees of supercooling, become the source of spiral growth [244]. Burton, Cabrera and Frank solved two problems: (a) the flow of the growth unit to the steps by the surface diffusion mechanism, and (b) the form of the stationary growth spirals when the surface diffusion is neglected.

Growth spirals were observed in a number of experimental works [245–250]. Moving steps and rotating spirals on the surface of crystals growing from solution were also observed recently [251,252].

The dependence of the growth rate on the supersaturation for spiral growth and two-dimensional nucleation growth was experimentally studied [253]. $R \sim (\Delta\mu)^2$ at low degrees of supercooling and $R \sim \Delta\mu$ at high degrees of supercooling.

Near the interface having low atomic roughness, the distance between the sites which have a higher binding energy to the growth unit (i.e. the distance between the kink sites) is high with respect to the molecular dimensions. Diffusion must therefore be included in the kinetic models [254]. Diffusion to growth sites can occur in the adsorption states of the surface (surface diffusion), directly through the surface layer of the parent phase (volume diffusion), or simultaneously by surface and volume diffusion.

Burton, Cabrera and Frank assumed that the limiting growth mechanism is surface diffusion, and they determined the growth rate R for the case of parallel equidistant steps [202]. They obtained the result $R \sim \Delta\mu^2$ at low levels of supersaturation $\Delta\mu$ and $R \sim \Delta\mu$ at higher levels of supersaturation. Mullins and Hirth applied a generalized form of the BCF (Burton, Cabrera and Frank) theory of equidistant steps to non-equidistant steps [255].

The Chernov model of bulk diffusion gives the same qualitative results for the dependence of growth rate R on supersaturation $\Delta\mu$ [256]. Chernov assumed that the distance between neighboring kink sites is sufficiently small that the edge of the steps can be considered as a linear continuous region where growth units can be involved and the concentration profile depends on the distance from the crystal surface and from the step position.

Gilmer, Ghez and Cabrera included the influence of bulk and surface diffusion [257], and this model was used for derivation of the dependence of growth rate on supersaturation [258]. $R \sim \Delta\mu^2$ at low levels of supersaturation and $R \sim \Delta\mu$ at high levels of supersaturation.

In the case of the atomically rough surface of the phase interface, the site of contact on the crystal surface is simultaneously the growth site, and

surface diffusion and actual interface morphology can be neglected. The Wilson–Frenkel model assumed that the transition rate of the molecules from the crystal to the parent phase reaches an equilibrium value (it is in fact higher). They further assumed that all surface sites are simultaneously growth sites (i.e. surface diffusion is infinitely fast), giving the upper limit of the growth rate [254]. In fact, the surface is never "perfectly" rough. $R \sim \Delta\mu$ at low supercooling $\Delta\mu$.

Most of the models of equilibrium structure and growth of the crystal surface used the so-called solid-on-solid (SOS) model of the interface [259–261]. In this model overhangs are not permitted, and hence the crystal can be considered as a collection of interacting columns perpendicular to the surface. (The SOS model is thus a subclass of the Ising model.) Growth is achieved by the transition of molecules from the melt to the solid phase, and vice versa (the effects of surface diffusion are neglected). The influence of the difference in structure between the liquid and solid phases at the phase interface is investigated in ref. 262. While the atoms are randomly adsorbed on the surface, the probability of transition of the adsorbed atoms from the crystal surface to the parent phase depends on their environment. Various approximations were used for the interaction of the adsorbed atoms with their environment [263–265], and these may be compared with the Monte Carlo results [266,267]. It follows from Monte Carlo simulation that linear growth kinetics occur when Jackson's factor $\alpha < \alpha^R = 3.2$, and non-linear growth kinetics occur when $\alpha > \alpha^R$. This may be fitted in principle to two-dimension nucleation curves of the birth and spread model [252]. The value α^R corresponds to the roughening temperature (it differs from the critical value $\alpha^R = 2$ established by Jackson). Gilmer, on the basis of Monte Carlo simulation, established the growth rate dependence on supersaturation for surfaces with screw dislocations [268]. Initially growth by the mechanism of spiral growth occurs (for $\alpha > \alpha^R$ at low supersaturation), but at higher supersaturation spiral growth and two-dimensional nucleation occur simultaneously. Two-dimensional nucleation becomes faster than spiral growth for $\Delta\mu/k_BT \approx 2.8$, but the change in dominant growth mechanism strongly depends on surface diffusion [272]. For $\alpha > \alpha^R = 3.2$ continuous or "normal" growth occurs, where the upper limit of the surface diffusion is given by the Wilson–Frenkel model.

Kinetic models involving surface diffusion were widely applied to binary and multicomponent systems. Kinetic coefficients and growth rate dependence on the model and growth parameters for one-component and two-component metal systems were computed in refs. 269–273.

Numerical models of growth on the phase interface (which are still used more often today) are studied in refs. 274–285 and 288. On the basis of these computations, the phase interface structure was studied. The probability of transition of the atoms from the liquid to the solid phase is an important parameter in these computations. The numerical computations

use solution of the Fokker–Planck equation or the Monte Carlo method. On the basis of these methods, the influence of impurities on crystal growth was studied [281,286]. The molecular dynamics method, where the classical equation of motion for the molecular system is solved and the change in mean positions followed, belongs among these methods. The phase interface within the framework of this method is investigated in refs. 216 and 287–290.

As a point of interest we can now introduce here quantum-mechanical computations of the phase interface motion—the increase or decrease of atoms on the phase interface. These computation methods are used in the description of ^{4}He crystallization at $T \to 0$ K. Under such conditions the quantum effects appear as, for example, Kapica's temperature jump on the phase interface [277].

Crystal growth kinetics have a great influence on crystal quality. For instance, crystals grown on perfect smooth surfaces (requiring high supersaturation and supercooling) will differ from crystals grown on a different surface with a much lower degree of supercooling [234]. It is therefore important to study kinetic processes at the phase interface.

The growth process at the phase interface is also influenced by mass and energy transport in the system. Hitherto we were only looking at phase transformation kinetics near the phase interface. We are now interested in the entire solidification process of binary melts at the phase interface. The composition (concentration) of the solid phase at the phase interface as a function of a time will be followed. In principle, three cases are distinguishable: (i) a solidification process near thermodynamic equilibrium (at very low supercooling); (ii) a stationary regime with non-zero supercooling, which is time independent (like concentration of a liquid phase) and occurs at a constant rate; (iii) a non-stationary regime where undercooling and concentration of the liquid and solid phases at the phase interface are time dependent, as is the solidification rate.

We can use equilibrium phase diagrams (see refs. 25 and 291) to describe processes of the first case, which are common with slow cooling and fast phase transformation kinetics (e.g. for the cooling rates of the metals up to 10^3 K s^{-1}). The influence of temperature fluctuations on growth at the phase interface involving equilibrium phase diagrams was studied in ref. 292.

So-called kinetic phase diagrams (for the theoretical basis see Section V) for a description of stationary non-equilibrium processes where equilibrium phase diagrams do not suffice were developed. These phase diagrams depend on the experimental conditions of the solidification process, such as, for example, cooling rate, supercooling at the phase interface, etc. The influence of individual parameters on the kinetic phase diagrams in the model cases was investigated (see refs. 270–273 and 293–308).

Figure 15 shows the influence of growth rate on the position and shape of

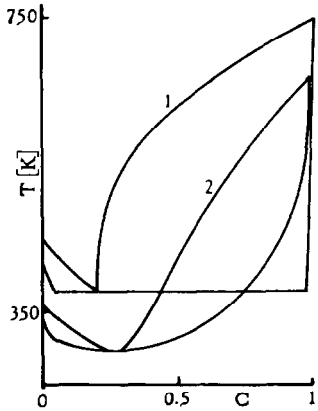

Fig. 15. Kinetic phase diagram for various growth rates R (the model example): 1, $R = 0$; 2, $R = 0.2$ (relative value). See ref. 303.

the phase diagram (according to theory from ref. 303). It can be shown that the phase diagram shifts to lower temperatures with increasing growth rate and the diagram shape may even change (from eutectic to cigar shape, see for example ref. 303). Figure 16 shows the dependence of growth rate on supercooling in this case (see ref. 271).

For non-stationary processes a completely different situation occurs. Here phase diagrams can not be used because the concentration of the solid and liquid phases and the degree of supercooling change with time. These depend both on the given material and on the course of the entire process. Therefore, the description of such a solidification process is necessarily complex. Such a complex description of non-stationary processes was developed within the framework of the stochastic theory of solidification (see ref. 273) for some model situations of Cu–Ni alloy solidification. The solidification process was modeled as the solidification of a melt column, which is cooled down at a constant rate at one end. Mass and energy transport occurs only by diffusion (if we neglect convection). Within the framework of this model, the time dependence of the concentration of the liquid phase $C_{Lr}(t)$ and that of the solid phase $C_{Sr}(t)$ on the phase interface, that of the undercooling $\Delta T(t)$ on the phase interface (corresponding to the equilibrium solidification temperature for the liquid phase of concentration $C_{Lr}(t)$) and the solidification rate $R(t)$ were obtained (see ref. 273). The results are shown in Fig. 17. The stated values at various cooling rates φ, the diffusion coefficients in the liquid phase D^L and the parameters connected with the rate of phase transformation kinetics in the model case is given in Table 3. Qualitative changes of the stated parameters with changes in the parameters φ, D^L and ν are given in Table 4 (see ref. 273). In the case of Cu–Ni alloy solidification, it was shown within the framework of the given model that the process behaves as a stationary one up to a cooling rate of 10^3 K s^{-1} under conditions which are very close to equilibrium ones. The

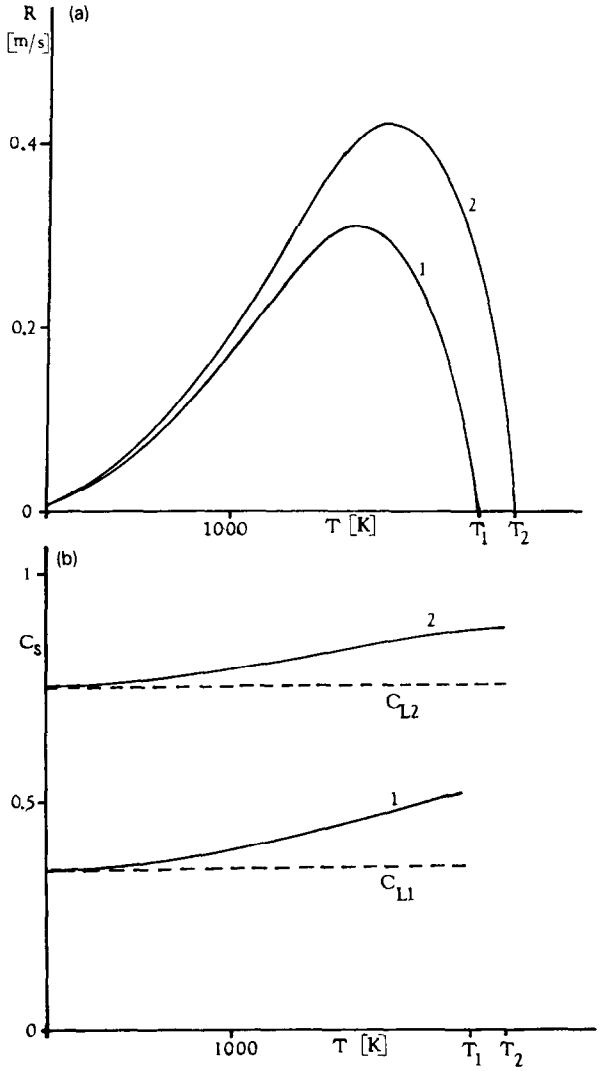

Fig. 16. (a) Dependence of the stationary solidification rate R on the undercooling for Cu–Ni alloy and concentration of liquid phase C_L: 1, $C_{L1} = 0.35$; 2, $C_{L2} = 0.75$. T_1 and T_2 are equilibrium temperatures of solidification of the alloy with concentration C_{L1} and C_{L2} respectively. (b) Dependence of the stationary concentration of solid phase C_S on undercooling for Cu–Ni alloy and concentration of liquid phase C_L: 1, $C_{L1} = 0.35$; 2, $C_{L2} = 0.75$.

process is non-stationary at higher cooling rates. In this way we can estimate the limit of applicability for equilibrium and kinetic phase diagrams.

It follows from the analysis given how various dependences of the new phase composition can be obtained if the experimental conditions of its formation are changed. At the same time, a change in structure would occur, an amorphous phase would be formed, the metastable phase would freeze, etc. At present we are restricting ourselves to temperature changes. It would

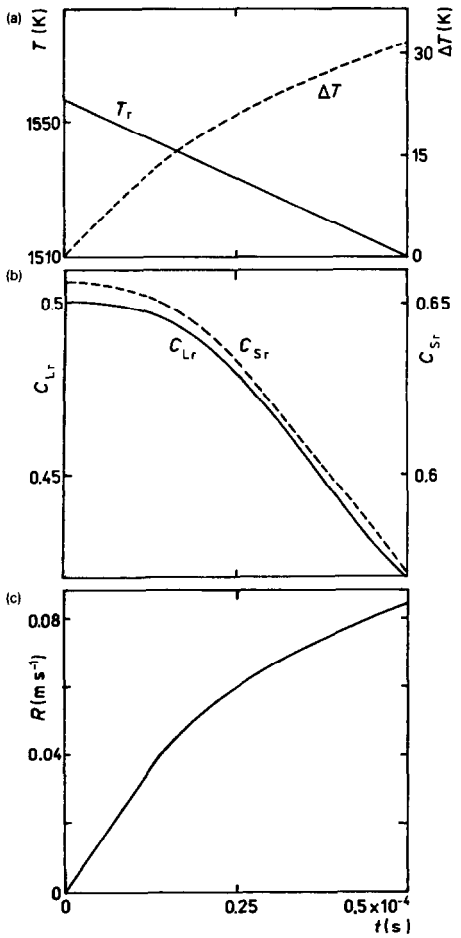

Fig. 17. Time dependences of parameters (a) ΔT (undercooling at the solidification front) and (b) T_r, C_{Lr} and C_{Sr} and (c) the solidification rate R for cooling rate $\varphi = 10^6$ K s^{-1}, $\nu = 3\times10^{10}$ s^{-1} and $D^L = 0.73\times10^{-7}$ m^2 s^{-1} (the diffusion coefficient in the liquid phase).

TABLE 3

The illustration of the calculations of the solidification of the 50 Cu–50 Ni alloy for the chosen values of parameters ($t = 10^{-4}$ s)

φ (K s^{-1})	ν (s^{-1})	D^L (m^2 s^{-1})	T_r (K)	C_{Lr}	C_{Sr}	R (m s^{-1})	C^e_{Sr}	T^e_r (K)
10^3	3×10^{10}	7.3×10^{-8}	1556.9	0.4999	0.6557	7.41×10^{-4}	0.6558	1557.1
10^3	3×10^{10}	7.3×10^{-4}	1556.9	0.5000	0.6557	7.63×10^{-4}	0.6558	1557.1
10^3	3×10^{6}	7.3×10^{-8}	1556.9	0.5000	0.6558	7.68×10^{-8}	0.6558	1557.1
10^6	3×10^{10}	7.3×10^{-8}	1461.6	0.3254	0.4749	0.159	0.4788	1520.5
10^6	3×10^{10}	7.3×10^{-4}	1476.8	0.4999	0.6451	0.206	0.6558	1557.1
10^6	3×10^{6}	7.3×10^{-8}	1455	0.5000	0.6430	2.47×10^{-5}	0.6558	1557.1

$C^e_{Sr}(t)$ is the equilibrium solid phase concentration at the liquid phase concentration $C_{Lr}(t)$.
$T^e_r(t)$ is the equilibrium temperature of melting at the liquid phase concentration $C_{Lr}(t)$.

TABLE 4

The qualitative dependences of the parameters characteristic of the solidification conditions on φ, ν and D^L

Increase of value	Change of value				
	T_r	ΔT	C_{Lr}	ΔC	R
φ	Intensive decrease	Increase	Decrease	Decrease	Nonlinear increase
D^L	Decrease	Increase	Increase	Decrease	Increase
ν	Increase to equilibrium value	Decrease to zero	Decrease	Increase	Increase

be necessary to include in the theory the influence of pressure changes, changes in external fields, etc., where we would expect new effects under extremum conditions of new phase formation. We also did not investigate the changes which occur during cooling of the liquid phase (complexes, clusters, viscosity changes, etc.). It is thus possible to say that we are at the beginning of construction of theory for solidification processes. The basis of this theory will be summarized in the Section V below. At present, direct experiments, in which it is possible to follow the given processes, are not possible although the observed effects are strongly connected with the quality of the phase formed.

V. ANALYSIS OF RECENT THEORETICAL DESCRIPTIONS OF PHASE TRANSFORMATIONS

In order to construct a theory of phase transitions, we must consider processes which occur during phase transformation and which influence the results of the entire process. These may be divided into several groups.

(1) Primarily, this is a question about phase changes. Thus we must know the state and composition of the mother phase (liquid, gas, etc.), determine the conditions (pressure, temperature, etc.) under which the new phase forms in the system and determine its structure and composition.

(2) The new phase forms gradually in the system rather than instantaneously. We may observe the time evolution of the phase transformation, especially as a dependence on external conditions (thus the kinetics of phase transformation). At the same time, we must be aware that phase transformation occurs in two different steps. In the first stage, the nucleus of the new phase forms in the mother phase and does not constitute the region of another phase. Nucleation theory deals with this process. In the second stage, the growth of the new phase occurs at the interface (solidification

front), thus the new phase grows into the mother phase from the part of the new phase which already exists.

(3) The conditions at the point at which the phase transformation occurs are determined by energy and mass transport in the system. We must thus study the temperature and concentration distribution in the system and their changes with time in connection with initial and boundary conditions.

We shall now return to the particular points above and briefly estimate the results achieved in the theory relating to the applications considered.

V.1. Equilibrium and metastable phases

Phenomenological thermodynamics [27,309,310] deals with the conditions of phase transformation and the equilibrium coexistence of phases. This theory considers that phase transformation occurs at one point (e.g. a certain temperature and pressure) in the entire system and that the phase transformation is characterized by the behavior of the thermodynamic values (Gibbs potential, free energy, entropy, etc.) in the vicinity of the phase transformation point. The equilibrium phase corresponds to the minimum of the Gibbs potential. Phenomenological thermodynamics studies the static properties of the system.

As regards the equilibrium coexistence of phases, the well-known condition of equality of chemical potentials of different phases was derived at constant temperature and pressure in the system.

Phenomenological thermodynamics is based on the behavior of thermodynamic potentials. It is thus necessary to know or to model the dependences of, for example, the Gibbs energy G on temperature, on the intensity of external fields, on concentration or on the order parameter η which characterizes the new phase (e.g. change in concentration, magnetization, etc.). Most frequently used is the Landau–Ginzburg relation [311]

$$G = \int_V \left(G_0 + \alpha_G \eta^2 + \beta_G \eta^4 + \gamma_G \operatorname{grad} \eta\right) \mathrm{d}x^3 \tag{26}$$

where V is the volume of the system and G_0, α_G, β_G and γ_G are coefficients which depend on the temperature and space coordinates. This form of potential G describes the behavior of the system in the vicinity of the phase transformation. It is used to describe the nucleation of metastable states and the phase transition dynamics. In this method the equilibrium and metastable states are determined from the condition $\delta G = 0$. The stable states correspond to the absolute and metastable states to a local extremum of G. These conditions are assumed at a given temperature and at constant boundary conditions. Thus, for example, the concentration distribution in the system with a non-homogeneous distribution of temperature may be determined. The Landau–Ginzburg form of the Gibbs potential is used in

renormalization group theory [312], which is at present the most successful theory of phase transitions.

The renormalization group is the group of symmetry operations which act on the space of a-parameters of the Hamiltonian of the system. These operations are determined in the following way. The volume of the system is first divided into blocks of volume L_R^3, in which the values of the Hamiltonian parameters are substituted for their average values, and then the volume is reduced in the ratio $1/L_R$. We thus obtain the new Hamiltonian for our system with new values of the parameters a'. The group of operations R_L: $a \to a'$ is the renormalization group. The points $a^\star$ for which $R_L a^\star = a^\star$ are the stationary points. All a for which $\lim_{L_R \to \infty} R_L a = a^\star$ form the critical surface. The renormalization group method is based on the main hypothesis that the parameters of the Hamiltonian at the critical point T_c of the phase transformation are located on the critical surface. This is connected with the fact that at the critical point the correlation length of the order parameter exceeds all limits. Solution of the model concentrates on a description of the critical surface. The renormalization group method was formulated for quantum systems and can be used for the description of phase transitions in these systems.

The dynamic renormalization group method enables us to observe the time dependence of the order parameter η and to include the fluctuations of η in the kinetic equations by Langeven's method (see below).

For the determination of thermodynamic potentials of simple systems we may use classical or quantum statistical physics, using the partition function of the system [313] and the Hamiltonian of the system.

As regards the modeling of the dependence of the Gibbs potential on the constitution of binary systems, which is used for the construction of equilibrium phase diagrams, Table 2 shows the separate models. Deviations from ideal behavior of binary systems results in the existence of eutectic, peritectic or monotectic points in the phase diagrams [314]. Reference 315 deals with relations between interatomic forces and tip of the phase diagram; it was for example shown that a eutectic structure arises if the components A and B have different structures.

An interesting generalization of the thermodynamic description of phase transformation is the theory of diffuse phase transitions [316], which assumes that the phase transformation takes place in the temperature interval in which both phases exist in the system. The result of this assumption is new functions of the order parameter on temperature (e.g. magnetization in the vicinity of the Curie temperature in ferromagnetics, see ref. 317), the possibility of hysteresis during cyclic cooling or heating, or the non-singularity of the temperature dependence of heat capacity, susceptibility, etc.

These descriptions refer to the static equilibrium properties of the system. In spite of the indisputable successes of these theories and their wide extension, they are not in principle able to predict what phase or structure or

composition of new phase arises during the given experimental conditions. They give information about which states present in the equilibrium state of system can or cannot occur. The relaxation time of the transition of the system to this equilibrium state depends on the properties of the system and on the conditions of the process. Its value may be small (e.g. 10^{-13} s for metals) or large (e.g. thousands of years for glasses).

If we appreciate that the thermodynamic state of the system changes during non-isothermal conditions, it is clear that the kinetics of phase transformation plays the main role in phase transformation. If the phase transformation is more rapid, we may approach the thermodynamic equilibrium conditions. Cases may occur in which the slowness of the phase transformation can substantially influence the result of the process. In undercooled liquids, the metastable phases can freeze. It is thus necessary to study the metastable states of the system (which are determined by the local extrema of the thermodynamic potential) and the dynamics of their formation.

In connection with the modification of solid state surfaces by lasers, a new field of solid state physics is now developed. This is the theory of highly excited states of solid phases, which introduces new effects connected with highly excited states [318].

The indisputable benefit of a description of statics of the system is that we study the non-equilibrium conditions (undercooling, supersaturation, etc.), we must refer these to the equilibrium states which we must therefore know.

V.2. Kinetics of phase transformation

This field may be divided into nucleation processes and growth on the interface. These basic theories were analyzed in the Sections III and IV. The most recent results are now summarized.

Among modern theories which deal with nucleation, stochastic theory, the renormalization group method and field theories based on the Landau–Ginzburg potential are considered. Stochastic theory is successful with the Fokker–Planck equation (eqn. (6), where the coefficients c_n and e_n represent the probabilities of transition of an atom to or from the clusters. The function $F_n(t)$ represents the probability distribution of the existence of a cluster of a given volume in the system at time t [37,319–321]. The Lyapunov function of the most probable evolution of the system was used to determine the critical value of the nucleus, which is equivalent to the critical value of the nucleus in classical theories [321].

Modelling of the cluster growth by the Monte-Carlo method [322] within the framework of the Ising model pertains to these theories. The results are comparable with solutions of eqn. (6). Calculations within the framework of the dynamic renormalization group are given in ref. 323. The transforma-

tions over the space of coefficients of kinetic equations ($\partial_t C = \{\mathcal{H}, C\} + \xi$) form the dynamic renormalization group (ξ represents fluctuations in the system). This is an exact calculation of nucleation, but the results do not exceed the frame of calculations using theories mentioned, such as the calculations which use the Landau–Ginzburg potential in the Ising model [123–125,168,169,311,324]. These methods have an advantage over classical theories of nucleation, as they start from first principles and use a statistical description in the given model Hamiltonian. They describe the nucleus as a collective excitation in the saddle point. Fluctuations are given by the expansion about the critical nucleus.

To finish, we would like to mention that we number among our theories quantum mechanical calculations of cluster states, their energy and structure which corresponds to the minimum energy, etc. [325,326].

We can complete our review of the theory of growth at the interface with several interesting results. The Monte-Carlo method was used in a study of the structure and composition of the solid phase during epitaxial growth on a substrate [327]. Here it was assumed that the intermolecular forces acting on the substrate were not additive, but depended on the relative cover of the surface by the new phase. The structure and composition of the surface phase depends on the intermolecular forces.

The motion of the interface has been studied using field methods based on the Ginzburg–Landau equation: in the region of equilibrium the change with time of the order parameter $\eta(r)$ is equal to the product of the kinetic coefficient D and the variation in free energy F with respect to η [328]

$$\frac{\partial \eta(r)}{\partial t} = -D\frac{\partial F}{\partial \eta} \tag{27}$$

The coefficient D and the energy F have been modelled at constant temperature. A similar equation was used in ref. 329 to study the order parameter changes under constant rate of interface motion (in the stationary case)

$$0 = \frac{\partial \eta}{\partial t} = -D\frac{\partial F}{\partial \eta} - R\frac{\partial \eta}{\partial x} \tag{28}$$

The Landau–Ginzburg expansion was used for determination of the free energy F. It was shown that a critical rate R exists, above which non-ordered phase growth occurs. This contributes to the kinetic phase diagram.

Within the framework of linear stability theory there are works on the stability to shape perturbation of the plane interface in binary systems [314,330–340]. On the basis of this analysis stability conditions were derived, but they use equilibrium phase diagrams at the interface and assume known gradients of temperature and concentration at the interface.

The term linear stability theory is understood to mean the stability of equations which describe the stationary or equilibrium state of the system

(the balance equations using the boundary and initial conditions) with respect to an arbitrary small perturbation u (higher powers of u are neglected). If for some perturbation growth is advantageous (u fulfils the basic equations), then the amplitude of this perturbation increases with time and the interface is unstable to this perturbation [341]. Linear analysis of the interface stability (neglecting convection) shows that the plane interface is stable if

$$\frac{\mathscr{G}^{\star}}{m_C \mathscr{G}_C} > 1 \tag{29}$$

for small growth rates, where

$$\mathscr{G}^{\star} = (k_S \mathscr{G}_S + k_L \mathscr{G}_L)/(k_L + k_S) \tag{30}$$

(the modified criterion of undercooling). k_L and k_S are heat conductivity coefficients in the liquid and solid phases, $\mathscr{G}_S$ and $\mathscr{G}_L$ are the temperature gradients at the interface in the solid or liquid phases, $\mathscr{G}_C$ is the concentration gradient at the interface in the liquid phase and m_C is the slope of a plot of the equilibrium melting temperature versus the concentration of the liquid phase.

This simple relation was improved by many authors (see review, ref. 336). The influence of convection and growth of dendrites on interface stability is presented in ref. 336. The influence of material anisotropy on interface stability and the formation and selection of figures (different structures and textures) during solidification is analyzed in ref. 338. The kinetics of phase transformation are neglected in all these models. The influence of radiation heat transport on interface stability in semitransparent materials is given in ref. 342. The morphological oscillation instabilities during rapid cooling were studied in ref. 330, where the influence of diffusion on interface stability was demonstrated.

In ref. 183 the motion of the interface during crystal growth was explained as expansion of the soliton wave in the system. In this paper, stochastic theory was used for a description of the evolution of the system. A constant temperature was assumed.

We have summarized two main ways of describing the kinetics of phase transformation—nucleation and growth on the interface. In every system, however, the phase transformation occurs with both phenomena—each supercritical nucleus which forms in the system grows. The most complete description of nucleation processes and subsequent growth is given in ref. 324, which is based on phenomenological field theory using the Landau–Ginzburg form of the free energy. The dynamic model of binary alloys is based on the following kinetic equation [311]

$$\partial_t \eta = \{\mathscr{H}, \eta(t)\} \tag{31}$$

It has been shown that the Hamiltonian of the system must include interactions with the surrounding bath as well as the energy of the system

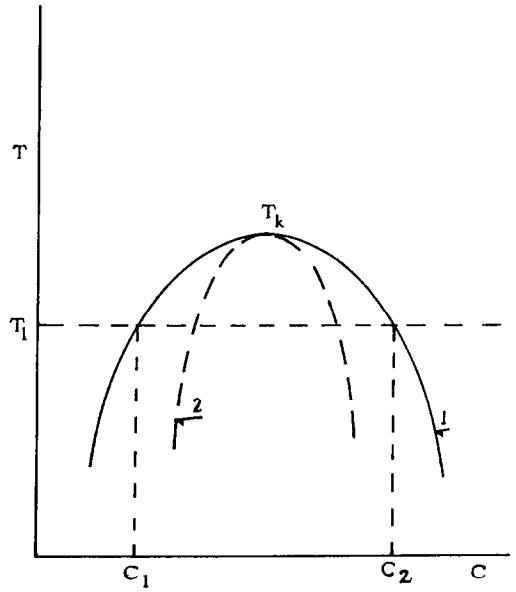

Fig. 18. Binary phase diagram with immiscibility curve (1) and spinodal curve (2). At temperature T_1 phases with concentration C_1 and C_2 are in equilibrium. T_k is the critical temperature of the phase decomposition.

(e.g. in the Landau–Ginzburg form) in order to enable us to describe phase transformations.

Equation (31) is the basic equation of the dynamic renormalization group method, although these methods were developed at a constant temperature in the system.

Besides these developments of the kinetics of phase transformation (nucleation and growth at the interface), the study of phase transformation kinetics is also developed using other theories. The most important results are summarized below.

First, if the system is in an unstable state, i.e. in a state below the spinodal curve (the curve defined by the equation $(\partial^2 G/\partial \eta^2) = 0$), the mechanism of phase transformation is not nucleation. The system decomposes spontaneously throughout the entire bulk. This process has been described using spinodal decomposition theory [343]. The system is unstable to small fluctuations of the order parameter. Usually, the system must be strongly undercooled (see Fig. 18).

Another method, which is based on the time changes of phases, is the molecular dynamics method. Here, the effect of changes of temperature with time on the ordering of molecules may be observed. The temperature is simulated by limiting the bulk kinetic energy of the system. The molecular dynamics method is very demanding in terms of numerical calculations. It is limited partly by the number of interacted molecules and partly by the

approximation of the interaction forces (mostly using the Lennard–Jones potential) [37].

Recently functional density methods have become popular in classical statistical mechanics. The processes of solidification of melts during nucleation or growth at the solidification front can be described using first principles [344,345]. This method is based on the assumption that the thermodynamic values (e.g. the free energy of the system) can be expressed as functions of the mean (equilibrium) density of particles $\rho_r(\vec{r})$. This density, as a function of coordinate $\vec{r}$, is constant in the liquid phase and is a periodic function in the crystalline phase. This change in density ρ_r represents the phase transition. In calculations the temperature is constant and the structure of the solid phase is known. The choice of potential energy of atoms in the system is also important. Usually, the Lennard–Jones potential is used. On the basis of the known form of the Hamiltonian of the system $\mathscr{H}$ (which depends on the density of atoms), kinetic equations for the mean density of atoms may be derived

$$\rho_r(\vec{r}) = Z^{-1} Tr\{ \rho_m(\vec{r}) \exp[-\beta(\mathscr{H} - \mu N)] \} \tag{32}$$

where the partition function Z has the form

$$Z = Tr \exp[-\beta(\mathscr{H} - \mu N)] \tag{33}$$

$\beta = 1/k_B T$ and μ is the chemical potential. The microscopic density of atoms is

$$\rho_m(\vec{r}) = \sum_{i=1}^{N} \delta(\vec{r} - \vec{r}_i) \tag{34}$$

$\vec{r}_i$ is the position of the ith particle. It can be shown that the free energy F of the system is a function of $\rho_r(\vec{r})$ and

$$\rho_r(\vec{r}) = \exp(\beta\mu + c(\vec{r})) \tag{35}$$

where $c(\vec{r})$ is the single-particle direct correlation function, for which many approximations were used (it depends on the potential energy of atoms). Solution of this problem enables us to determine the density distribution in a system and to determine the interface. However, even if this method is exact, it cannot include all phenomena which occur at the interface and it cannot observe processes which are non-isothermal.

The modern method of fractal geometry, where phase transformation evolution is studied, has the same imperfections [346,347]. Fractal systems are geometrical formations which are similar. An important fact is that the fractal dimension of these formations is different from the topological dimension, and can be different from the integral value. Different growth models apply to clusters or interfaces with different fractal dimensions, which characterize the shape of the clusters or the roughness of the interface [348,349].

V.3. Transport of mass and energy in the system

Transport of mass and energy in a system essentially occurs by two processes, diffusion and convection. In theory, the balance equations of mass, energy and momentum describe transport [314]. Balance equations are normally used in the local form.

The mass balance equation is (continuity equation)

$$\frac{\partial \rho_j}{\partial t} = -\nabla\left(\rho_j \vec{v}_{\text{con}} + \vec{j}_j\right) \tag{36}$$

where ρ_j is the density of mass of the jth component, $\vec{j}_j$ is the diffusion flux (given by Fick's relation) and $\vec{v}_{\text{con}}$ is the mean velocity of convection.

The energy balance is given by

$$\frac{\partial}{\partial t}\rho\left(U + 0.5v_{\text{con}}^2\right) = -\nabla\left\{\rho\left(U + 0.5v_{\text{con}}^2\right)\vec{v}_{\text{con}} + \vec{q} + \left[\Pi \cdot \vec{v}_{\text{con}}\right]\right\} + \sum_j \vec{n}_j \vec{g}_j + Q \tag{37}$$

where ρ is the total density of mass, U is the internal energy per unit mass, $\vec{q}$ is the diffusion flux of heat (given by Fick's relation), Π is the tensor of pressure, $\vec{g}_j$ is the external field which act on a unit mass of the jth component, $\vec{n}_j$ is the total flux of the jth component and Q is the source of energy.

The momentum balance equation (Navier–Stokes equation) is

$$\frac{\partial}{\partial t}\rho \vec{v}_{\text{con}} = -\nabla\left\{\rho\left(\vec{v}_{\text{con}} \cdot \vec{v}_{\text{con}}\right) + \Pi\right\} + \sum_j \rho_j \vec{g}_j \tag{38}$$

$(\vec{v}_{\text{con}} \cdot \vec{v}_{\text{con}})$ is the tensor $v_{\text{con}}^{IJ} = v_{\text{con}}^{I} v_{\text{con}}^{J}$. At high temperatures, radiation heat transport must be considered [350].

Diffusion processes may be described using the linear theory of non-equilibrium processes, where the fluxes are proportional to the thermodynamical forces, temperature gradient, chemical potential, etc. We may thus obtain the known equations of heat conductivity

$$k_{\text{L,S}} \frac{\partial^2 T}{\partial x^2} + Q_T(x) = \frac{\partial T}{\partial t} \tag{39}$$

where $Q_T(x)$ is the source of heat owing to the release of latent heat at the interface.

The diffusion equation for the concentration C has the form

$$D^{\text{L}} \frac{\partial^2 C}{\partial x^2} + Q_C(x) = \frac{\partial C}{\partial t} \tag{40}$$

where $Q_C(x)$ is the source of concentration owing to phase transformation, chemical reactions, etc.

The solution of these equations strongly depends on the boundary and initial conditions. During the solidification process, the boundary conditions at the solidification front must be specified. In the case of the heat conductivity equation this means calculating the latent heat of the phase transition (Stefan's condition). In the case of the diffusion equation the separation of one component as a consequence of different concentrations of the liquid and solid phases must be calculated. We must thus know the phase diagram for the processes at the interface which form the boundary conditions. A few papers exist which deal with measurements of the temperature at the interface which determines the processes of phase transformation (see, for example, ref. 351). In the case of high temperature gradients in the system, non-linear dependence of heat fluxes on temperature gradients can be dominant [358]. References 353–365 deal with calculations of temperature distribution during the crystal growth process under given experimental conditions. References 172–177 and 366–372 deal with solution of the diffusion equation during the solidification process. An analysis of the influence of convection on solidification was given in Section II above.

V.4. Complex descriptions of phase transformation kinetics

Theories dealing with kinetic phase transformation are mentioned above. They were divided into theories of formation of a new phase, theories of growth at the interface and theories of mass and energy transport in the system. In order to predict the result of the experimental process under given initial and boundary conditions, we must construct a theory which takes all these aspects of phase transformation into account. The kinetic conditions of growth form the boundary conditions for energy, mass and momentum balance and influence the temperature and concentration distributions in the system. On the other hand, transport properties of the melt determine the conditions at the phase interface, and so influence phase transformation kinetics.

There are in principle three cases: solidification can occur near conditions of thermodynamic equilibrium (very low degrees of undercooling); a stationary regime can occur with non-zero undercooling, which is constant with respect to time (as is the concentration of the liquid phase on the interface and the growth rate) and eventually a non-stationary regime can occur, in which case the undercooling, the concentration of the liquid and solid phases on the interface and the growth rate are dependent on time.

To describe the first types of process, which are common with low cooling rates of materials with rapid phase transformation kinetics (e.g. cooling of metals with cooling rates up to 10^3 K s^{-1} [273]), equilibrium phase diagrams at the phase interface may be used. Under these conditions solution of Stefan's problem can be used [340,367,373–376] (for a summary of numeri-

cal methods see ref. 377), where the phase interface coincides with a defined isotherm (e.g. the equilibrium melting temperature or the known undercooling, etc.). Convection is usually neglected. The influence of radiation heat transport is summarized in ref. 378. Recently, growth rate as a function of undercooling has been incorporated into this known method. In the case of binary systems, the validity of equilibrium phase diagrams is assumed to be the boundary condition at the interface for the concentration distribution in the solid phase. The set of equations is completed by the diffusion equation [352,367,370].

The conception of kinetic phase diagrams (which depend on the experimental conditions of solidification [304,306], see Section IV) was developed in order to describe stationary non-equilibrium processes, where equilibrium phase diagrams cannot be used. In these models, constant temperature and concentration at the phase interface is assumed. The transport equations (in contrast to Stefan's problem) are not solved. All theories of growth at the solidification front and thermodynamic theories of the solidification front (presented in Section IV) apply to this category.

Theories which describe the evolution of the solidification front using the solution of kinetic equations for the distribution function $g(\xi_i, C_i, t)$, where i indicates the position of the observed particle in the system (e.g. the point of the Kossel lattice), ξ_i indicates if the atom in the ith position is in the solid or liquid phase and C_i indicates the component to which the atom belongs (see refs. 293, 295, 303–308 and 379–384), in the stationary regime (i.e. the temperature in the system is constant) have the same restrictions. Here, elementary events as diffusion, adsorption or emission of atoms at the interface (which depend on temperature and on the change of system energy during these events) are considered. The main aim of these theories is to construct kinetic phase diagrams in the stationary regime of solidification.

Other calculations are based on the Monte-Carlo method [297,300,302, 303,385–388], where growth of the solid phase is simulated numerically.

Non-equilibrium thermodynamics were used in refs. 389 and 390 to study solidification, where the thermodynamic conditions of the solidification front motion and the composition of the solid phase under non-equilibrium conditions were derived from the energy, mass and momentum balance equations. Convection is also considered. In ref. 389 conditions of phase interface stability are formulated in diluted binary systems during growth under near-equilibrium conditions. In ref. 368 the influence of nonhomogeneity of composition of a binary system on the growth kinetics was studied. An equation for chemical potential in the nonhomogeneous system was derived here and the growth of the solid phase under non-equilibrium conditions was discussed in relation to kinetic processes on the solidification front and to diffusion in the liquid phase. In these papers, the processes of growth are connected with mass and heat transport in the system, but the kinetic coefficients of growth are assumed to be known constants and are

not connected with the growth process. A knowledge of phase diagrams is assumed (equilibrium phase diagrams were used).

The third case of nonstationary processes involves quite a different situation. Phase diagrams cannot be used because the concentrations of the liquid and solid phases and the undercooling at the interface all change with time, and depend on the properties of the material and on the course of the entire process. Thus, this process of solidification must be described in a complex manner. The transport of mass and energy in the system and the kinetics of phase transformation must be considered in a single model. This complex description of nonstationary processes was published in ref. 366, where the Monte-Carlo method was used to describe growth at the interface. At the same time, the temperature and concentration distributions in the binary system are simultaneously calculated. Calculations extend only as far as the growth of about 20 atomic layers.

Another approach to the complex description is one in which the temperature in the system is given and the kinetics of phase transformation are connected with the diffusion processes in the liquid phase [369,391]. In ref. 391 the boundary layer which modifies (with its potential) the concentration distribution in the vicinity of the interface is considered. The diffusion equation is solved using the assumption of a constant given growth rate R and a given temperature distribution in the system. It can be shown that the concentration of the solid phase C_S changes with R and approaches a mean value of the concentration of the liquid phase if $R \to \infty$. Two regimes of the growth are discussed; the kinetic and the diffusion regime.

The dependences of functions of R and C_S on C_{L_r} at the solidification front with the immiscibility region in binary systems are studied in ref. 369. The kinetics of phase transformation at the solidification front and diffusion in the liquid phase are given assumed values, and the temperature is constant in the system. The stability of stationary growth is studied in connection with phase diagrams, and oscillations of C_S at constant R are observed in the vicinity of the maximum of the immiscibility curve. The calculations, however, do not give the finishing touches to the kinetic phase diagrams.

References 270–273 and 392–400 deal with a similar complex description of the phase transition, where transport of heat and mass (in the diffusion regime only) are connected with kinetic processes at the interface in a single model. In this model, growth is assumed to be a stochastic process and the probability of a shift in the phase interface during a given time interval is calculated. This probability depends on the temperature distribution and on the kinetic processes at the phase interface. The position of the interface $X_r(t)$ at time t is given by the average value

$$X_r(t) = \int_{-\infty}^{\infty} x_r P(r,s,x_r,t)\, \mathrm{d}x_r \tag{41}$$

where $P(r,s,x_r,t)$ is the probability that at time t the interface is at x_r if at time s it was at position r (r and s are the initial conditions of the process). This stochastic theory was extended to the binary systems in refs. 270–273, 399 and 400, and the boundary conditions at the solidification front were determined in the form (kinetic phase diagrams)

$$C_S = \frac{C_L FA}{(1 - C_L)FB + C_L FA} \tag{42}$$

$$R = a_0 \nu P_1 [(1 - C_L)FB + C_L FA] \tag{43}$$

where C_S is the concentration in the solid phase, C_L is the concentration in the liquid phase, R is the solidification rate, a_0 is a lattice constant, ν is the frequency of thermal vibrations of molecules at the solidification front,

$$FA = 1 - \exp\left(-\frac{\Delta\mu^A}{k_B T}\right) \tag{44}$$

$$FB = 1 - \exp\left(-\frac{\Delta\mu^B}{k_B T}\right) \tag{45}$$

$$P_1 = \exp\left(-\frac{E_A}{k_B T}\right) \tag{46}$$

where T is the temperature at the solidification front, k_B is Boltzmann's constant, $\Delta\mu^i$ the difference in chemical potential between the ith component in the liquid and in the solid phase and E_A is the activation energy of transition of the molecule from the liquid to the solid phase.

The results from stochastic theory are in good agreement with results published in refs. 293–296, 301, 303–308 and 379–383 in the stationary regime of binary system solidification. Stochastic theory has even been used to describe non-stationary processes, and, in contrast to the Monte-Carlo method, it can describe the solidification of much greater than several tens of atomic layers (i.e., the growth of new phase is described on a macroscopic scale).

Because the structure and composition of the solid phase being formed is a result of the entire process of phase transformation (if this takes place far from thermodynamic equilibrium), it is obvious that only these complex models can accurately describe phase transformation.

The stochastic theory of nucleation [171,184,400], which looks at the probability of formation of a critical nucleus of a given concentration under non-stationary conditions, describes the nucleation process as a stochastic process which corresponds to the maximum probability of occurrence. It was used to describe nucleation processes in binary systems (Cu–Ni alloy), and kinetic phase diagrams of the nucleation process were derived (see Section III). The description of the kinetics of phase transformation at the solidification front can be combined with the nucleation process using

stochastic theory [400]. This theory enables us to observe the course of a wide spectrum of nonstationary non-equilibrium processes.

VI. CONCLUSIONS

Earlier in this paper several techniques were introduced which produce materials in a metastable state and for which the change in temperature is characteristic. If we can construct the theory of these processes, we must be able to predict the structure and composition of the new phase on the basis of knowledge of the mother material and the boundary and initial conditions of the technique. The aim of these theories is to predict the technique and the mother material for given properties of the resulting material. Our theory must therefore cover all processes which are connected with phase transformation (see Section V).

Summarizing the information in Section V, where the results in this field were discussed in detail, it is obvious that only the Monte-Carlo calculations and stochastic theory [273,288,366,401] describe the entire problem in sufficient detail. Many theories of phase transformation deal only with the equilibrium coexistence of phases. Other theories, even those that consider non-equilibrium conditions in the system, assume a given temperature and concentration in the system (which are mostly constant with respect to time). Theories which consider transport in the system assume equilibrium conditions at the phase interface or a given temperature in the system. These theories only partially solve the problem of finding the correct technique. On the other hand, they are acceptable and very successful for some techniques, e.g. we may consider equilibrium conditions at the solidification front during slow cooling. In other cases, diffusion processes in binary systems are decisive for evolution of the system and other effects may be neglected.

The success of these theories is connected with the solution of concrete technical problems. For example, it is very important to know the stability regions in the growth of eutectics of lamellar structure, or to determine the recrystallization rates of glasses using nucleation theories. The temperature distribution in the system influences thermal stress in the solid phase, and thus influences defect distribution. Kinetic phase diagrams advise us on which metastable phase is forming. The distribution of defects and impurities in crystals is connected with kinetic processes at the phase interface, etc.

However, under the extreme conditions of solidification, when metastable phases form, it is evident that equilibrium conditions do not obtain at the solidification front and we must consider the kinetics of phase transformation together with rapid changes in temperature and composition of the liquid phase. It is thus necessary to bring together both processes in a single theory. It is also necessary to realize that the stationary approximation is sufficient and that it is necessary to consider time-variable boundary condi-

tions. The theory should be able to describe nucleation and growth at the interface in a uniform way.

We now need to know which theoretical descriptions can be used to formulate a theory which fulfils our requirements. Because the processes under study are nonequilibrium processes it is necessary to use methods of nonequilibrium thermodynamics, and use the evolution theorem to determine the resulting structure [402–404]. We must, however, be aware that this theorem only holds if the boundary conditions are constant with respect to time, that its use is advantageous only in the case of stationary processes (e.g. the formation of dissipative structures) and not where variable boundary conditions are involved, and that the kinetic coefficients at the interface must be obtained experimentally [389,390].

For reasons which were discussed in Section IV, the following methods are unsuitable since the kinetics of phase transformation are not considered: Monte-Carlo calculations, the methods of molecular dynamics (here we may calculate only the growth of a few atomic layers), the method of density functions, the renormalization group method or field methods using the Landau–Ginzburg approximation. Neither can solution of Stefan's problem (where phase diagrams must be known) be used. These theories must be generalized so that they fulfil our requirements.

Further, I would like to emphasize that it is possible to use statistical methods to describe processes mentioned above relating to the advantages of molecular processes in phase transformation and to the existence and influence of fluctuations in thermodynamic values near the phase transformation point. The most general description would be solution of the Liouville equation for the density matrix operator (or solution of the generalized master equation [405]) using quantum mechanics and the reservoir density matrix in which temperature is a function of time [406,407]. With this theory we would be able to describe even non-Markovian processes. This method was, however, not used for the processes under study owing to the difficulty of the above-mentioned problems of considering many effects in the framework of a single model.

The new method, which uses a mathematical method of the stochastic processes and which fulfils our requirements, seems useful. This theory enables us to describe the processes of nucleation and growth at the interface in terms of a single model.

From the above-mentioned theoretical and experimental results it follows that study of phase transformation kinetics under nonequilibrium conditions is a rapidly developing branch of materials research, which is studied by physicists and technologists. Merely the attempt to obtain new materials, more perfect materials or pure materials with new properties leads us to a better determination and description of processes and to a better understanding of the course of phase transformation. The imperfection in the present state of the art lies in the nonsystematic experimental study of

processes which are far from equilibrium or under time-dependent boundary conditions.

Development of theory is also in its initial stages. In spite of partial successes (kinetic phase diagrams, the problems of interface stability, etc.) calculations of convection are complicated, and (for example) the question of the influence of external fields on phase transformation and the determination of surface energy and kinetic coefficients are not solved. Nevertheless, development in this field is taking place and closer contact between theory and experiment is necessary for solution of the problems outlined in this review. It is necessary to devote attention to the characterization of materials, to the study of phase transformation processes, and to the study of temperature fields which determine the entire process. This is necessarily connected with the development of thermal analysis.

PRINCIPAL SYMBOLS

A_n	surface of an n-atom cluster of new phase
a	parameters of the Hamiltonian of the system in renormalization group theory
a_0	lattice constant
$\mathrm{a}^\star$	stationary points of renormalization group
$c(\vec{r})$	single-particle direct correlation function
C_L	concentration of one component in binary system in liquid phase
$C_{\mathrm{L}r}$	concentration in liquid phase at the solidification front
c_n	number of atoms passing per unit time from the parent to the newly forming phase
C	concentration of one component in binary system
C_S	concentration of one component in binary system in solid phase
$C_{\mathrm{S}r}$	concentration in solid phase at the solidification front
D	kinetic coefficient in the Landau–Ginzburg equation
D^L	diffusion coefficient in liquid phase
E_A	activation energy of transition of a molecule from liquid to solid phase
E	electromotive force
e_n	number of atoms passing per unit time from the newly forming to parent phase
$\mathscr{F}$	Faraday constant
F	free energy of system
$F_n(t)$	distribution function of clusters of n atoms at time t
F_n^0	equilibrium distribution function of clusters
f_{hkl}	ratio of the number of nearest neighbors in the plane of crystal parallel to the interface and the bulk coordination number

G	Gibbs energy
$\mathscr{G}_C$	concentration gradient at interface in liquid phase
$\mathscr{G}_{S,L}$	temperature gradient at interface in solid or liquid phase
$g(\xi_i,c_i,t)$	distribution function of atoms of given component c_i and phase ξ_i at position i and time t
$\vec{g}_j$	external forces acting on the unit mass of the jth component
H	enthalpy of the system
$\mathscr{H}$	Hamiltonian of the system
h	Planck constant
$I(t)$	nucleation rate
$I_{A,B}$	flux of ion of components A and B
I_S	stationary nucleation rate
J_n	rate of n-atom cluster formation
$\vec{j}_j$	diffusion flux of jth component
k_B	Boltzmann constant
$k_{L,S}$	heat conductivity coefficient in liquid and solid phase, respectively
K_{DTA}	apparatus constant in DTA method
L	change of internal energy during phase transformation per atom
m	charge
m_C	derivation of the equilibrium solidification temperature as a function of concentration in melt
N	number of atoms in system
n	number of atoms in cluster
$\vec{n}_j$	total flux of jth component
$n^\star$	critical number of atoms in nucleus
$P(r,s,x,t)$	probability that the solidification front is in position x at time t; r and s are the initial conditions
$P_{A,B}$	partial pressures of components A and B
P_n	probability of n-atom cluster formation
Q	source of energy
Q_C	source of concentration
Q_T	source of heat
$\vec{q}$	diffusion flux of heat
R	growth rate at solidification front
$\vec{r}$	radius vector
S	entropy
T	temperature
T_E	equilibrium melting temperature
T_{Re}	reference temperature
Tr(A)	trace of matrix A
T_S	temperature of sample
(T_x,t_x)	point in T–T–T diagram corresponding to the minimum time for formation of the volume fraction X_d of the new phase

$\dot{T}_{\min}$	minimum cooling rate for glass formation
t	time
u	perturbation of the planar interface
U	internal energy per unit mass
$V(t)$	volume of the crystalline phase
V_0	volume of the parent phase
$v(t-t')$	volume at time t of the growing crystalline nucleus forming at time t'
v_{con}	average convection velocity
v_{m}	mean velocity of atoms
$X(t)$	volume fraction of the crystalline phase
$X_{\text{A,B}}$	atomic fraction of components A and B
$X_{\text{r}}(t)$	position of solidification front at time t
X	the maximum value of volume fraction of the crystalline phase in glasses
Z	partition function
z	Zeldovich factor

Greek letters

α	apparent degree of crystallization
α_j	Jackson factor
α^{R}	critical value of α_j
γ	surface shape factor
ΔG	change in Gibbs energy
ΔG^{ex}	change in excess Gibbs energy
$\Delta G_n(T)$	work needed for formation of an n-atom cluster at temperature T
$\Delta G_{n^*}^{\text{Het}}(t)$	$\Delta G_{n^*}(T)$ during heterogeneous nucleation
ΔC	$= C_{\text{S,}} - C_{\text{L,}}$
ΔH	change in enthalpy
ΔS	change in entropy
ΔT	undercooling
$\Delta \mu^i$	difference in chemical potentials of the liquid and solid phases of the ith component during phase transition
η	order parameter
ϑ	wetting angle
μ	chemical potential
$\mu^i_{\text{L,S}}$	chemical potential of ith component in liquid or solid phase
ν	frequency of thermal vibrations of molecules
ν_{k}	kinetic coefficient of phase transformation
Π	pressure tensor
ρ	total density
ρ_j	density of jth component

$\rho_r(\vec{r})$	equilibrium density of atoms
ρ_S	surface density of atoms
$\sigma(T)$	specific surface energy density
Φ	bonding energy of atoms
φ	cooling rate
Ω	interaction parameter

REFERENCES

1 E.M. Levin and H.F. McMurdie (Eds.), Phase Diagrams for Ceramics, American Ceramic Society, Columbus, 1964–1980.
2 J. Šesták, Thermophysical Properties of Solids, Elsevier, Amsterdam, 1984.
3 J. Šesták, Thermochim. Acta, 28 (1979) 197.
4 H.J. Seifert and G. Thiel, Thermochim. Acta, 100 (1986) 81; 110 (1987) 297.
5 O. Kubaschewski and C.B. Alcock, Metallurgical Thermochemistry, Pergamon, New York, 1979.
6 W. Hemminger and G. Höhne, Grundlagen der Kalorimetrie, Verlag-Chemie, Weinheim, 1979.
7 O. Kubaschewski, Thermochim. Acta, 22 (1978) 199.
8 W. Hemminger, Thermochim. Acta, 40 (1980) 41.
9 V. Pekárek, Chem. Listy Prague, 69 (1975) 787.
10 J. Velíšek, Chem. Listy Prague, 72 (1978) 801.
11 K.P. Komarek, Ber. Bunsenges. Phys. Chem., 81 (1977) 936.
12 O. Kubaschewski, Physica B, 103 (1981) 101.
13 B. Predal, Calphad, 6 (1982) 199.
14 G. Bruzzone, Thermochim. Acta, 96 (1985) 239.
15 W. Oelsen, K.H. Reiskamp and O. Oelsen, Arch. Eisenhüttenwes., 26 (1955) 263.
16 F. Sommer, Z. Metallkunde, 70 (1979) 545.
17 M. Notin, C. Cunat and J. Hertz, Thermochim. Acta, 33 (1979) 175.
18 W.D. Emmerich and H. Pfaffenberger, Thermochim. Acta, 93 (1985) 295.
19 T. Hebenkamp and R. Wüttenborst, Z. Metallkunde, 64 (1973) 69.
20 T. Hebenkamp and M. Manz, Z. Metallkunde, 65 (1974) 285.
21 H.E. Peltner and C. Herzig, Acta Metall., 29 (1981) 1107.
22 A. Nechel and S. Wagner, Ber. Bunsenges. Phys. Chem., 73 (1969) 210.
23 T. Ansara, Inst. Met. Rev., 24 (1979) 20.
24 H.L. Lukes, J. Weiss and E.T. Aenig, Calphad, 6 (1982) 229.
25 A.R. Miedema and G.W. Rathenau (Eds.), Proc. Int. Symp. Thermodynamics of Alloys, Delft, 1980, Physica B, 103 (1982) 182.
26 A.M. Alper (Ed.), Phase Diagrams, Vol. I-5, Academic Press, New York, 1970.
27 L. Kaufman and H. Bernstein, Computer Calculation of Phase Diagrams, Academic Press, New York, 1970.
28 P.J. Spencer and I. Barin, Mater. Eng. Appl., 1 (1979) 167.
29 Z. Pánek and V. Daněk, Silikáty (Prague), 21 (1977) 97; 30 (1986) 97.
30 J. Mailing and V. Jesenák, Silikáty (Prague), 29 (1985) 343; 30 (1986) 319.
31 I. Horsák and I. Sláma, Chem. Listy (Prague), 41 (1987) 23; 36 (1982) 311.
32 M. Nevřiva and K. Fisher, J. Cryst. Growth, 1988, in press.
33 P. Holba, Silikáty (Prague), 23 (1979) 193; 24 (1980) 100.
34 F. Sommer, Z. Metallkd., 73 (1982) 72; Ber. Bunsenges. Phys. Chem., 89 (1988) 571.
35 Z. Jiang, X. Hu and X. Zhao, J. Non-Cryst. Solids, 52 (1982) 235.

36 J. Šesták and Z. Chvoj, J. Therm. Anal., 32 (1987) 1645.
37 V.P. Skripov and V.P. Koverda, Spontaneous Crystallization of Undercooled Liquids, Nauka, Moscow, 1984 (in Russian).
38 J. Šesták, Thermochim. Acta, 95 (1985) 459.
39 J. Šesták, J. Therm. Anal., 33 (1988) 75.
40 J. Burke, The Kinetics of Phase Transformations in Metals, Pergamon, Oxford, 1965.
41 C.N.R. Rao and K.J. Rao, Phase Transitions in Solids, McGraw-Hill, Chatham, 1978.
42 J.W. Christian, The Theory of Transformations in Metals and Alloys, Pergamon, New York, 1975.
43 P.I.K. Onorato and D.R. Uhlmann, J. Non-Cryst. Solids, 22 (1976) 367.
44 G.P. Boswell, Mat. Res. Bull., 12 (1977) 331.
45 D. Domb and J.L. Lebowitz (Eds.), Phase Transitions and Critical Phenomena, Academic, London, 1983.
46 J.W. Cahn, in R.E. Mils, E. Asher and R.J. Jafer (Eds.), Critical Phenomena in Alloys, Magnets and Superconductors, McGraw-Hill, New York, 1971.
47 H.J. Güntherodt and H. Bech (Eds.), Glassy Metals I and II (Topics in Appl. Phys. 46 and 53) Springer-Verlag, Berlin, 1982, 1983.
48 R.W. Cahn, Chart. Mech. Eng., 33 (1986) 22.
49 W.J. Nellis, M.B. Maple and T.H. Geballe, Synthesis of Metastable Materials by High Dynamic Pressures, in Comm. Mater. Sci. Eng. Study, MRS, Pittsburg, 1986, p. 25.
50 W.J. Boetlinger and J.H. Perepezko, in S.K. Das and B.H. Kear (Eds.), Rapidly Solidified Alloys, TMS-AIME, Warrendale, PA, 1985.
51 F.E. Luborsky (Ed.), Amorphous Metallic Alloys, Butterworths, New York, 1983.
52 H.A. Davies, in B. Cantor (Ed.), Rapidly Quenched Metals III, Vol. 1, Brighton, 1978, p. 1.
53 H.S. Chen, Glassy Metals, Rep. Prog. Phys., 43 (1980) 353.
54 B.K. Kear, B.C. Giessen and M. Cohen (Eds.), Rapidly Solidified Amorphous and Crystalline Alloys, North-Holland, New York, 1982.
55 H.W. Bergmann and H.U. Fritsek (Eds.), Rapidly Solidified Metastable Materials, Symp. Proc., Boston, MRS, Pittsburg, 1983.
56 F.X. Kelly and L.H. Ungar, Phys. Rev. B, 34 (1986) 1746.
57 N. Sounders and A.P. Miodownik, J. Mater. Res., 1 (1986) 38.
58 P. Strimbord, D.R. Nelson and M. Roucheti, Phys. Rev. Lett., 47 (1981) 1297.
59 S. Moze and F. Yonezawa, J. Chem. Phys., 84 (1986) 1803.
60 R.J. Schaefer and L.A. Benderly, in Rapidly Solidified Alloys and their Mechanical and Magnetic Properties, MRS, Pittsburg, 1986.
61 S. Dattagupta and L.A. Turshi, Phys. Rev. Lett., 54 (1985) 2359.
62 J.C. Phillips, J. Mater. Res., 1 (1986) 1.
63 M.O. Tompson, P.S. Peerey, J.Y. Tsao and M.J. Aziz, Appl. Phys. Lett., 49 (1986) 558.
64 J.M. Poate, J. Cryst. Growth, 79 (1986) 549.
65 R.B. Hall, J. Phys. Chem., 91 (1987) 1007.
66 R.F. Wood and G.A. Geist, Phys. Rev. B, 34 (1986) 2606.
67 H. Wiedersich, Material Modification by Energetic Beams, in Comm. Mater. Sci. Eng. Study, MRS, Pittsburg, 1986, p. 15.
68 D.R. Uhlmann and N.J. Kreidl (Eds.), Glassforming Systems, Academic, New York, 1983.
69 A. Feltz, Amorphous and Glassforming Inorganic Solids, Akademic-Verlag, Berlin, 1983 (in German), Mir, Moscow, 1986 (in Russian).
70 J.D. Livingston, J. Cryst. Growth, 24–25 (1974) 94.
71 M. Nevřiva and J. Šesták, in Ž.D. Živković (Ed.), Thermal Analysis, Sci. Papers Univer. Bor, Technical University Press, Yugoslavia, 1984, p. 3.
72 F. Rosenberger, J. Cryst. Growth, 65 (1983) 91.

73 S.R. Corrill, G.B. McFadden, R.F. Boisvert and R.F. Seherta, J. Cryst. Growth, 69 (1984) 15.
74 R. Payret and T.D. Taylor, Computation Methods for Fluid Flow, Springer-Verlag, New York, 1983.
75 M.A. Azouni, Physicochem. Hydrodynam., 2 (1981) 295.
76 G. Müller, G. Neumann and W. Weber, J. Cryst. Growth, 70 (1985) 78.
77 C.J. Chang and R.A. Brown, J. Cryst. Growth, 63 (1983) 343; J. Comput. Phys., 53 (1984) 53.
78 D. Camel and J.J. Favier, J. Cryst. Growth, 67 (1984) 42; 67 (1984) 67.
79 M.J. Crochet, F.T. Geyling and J.J. van Schaftinger, J. Cryst. Growth, 65 (1983) 166.
80 O.I. Batizova, O.V. Pelevin and A.M. Sokolov, Izv. Akad. Nauk SSSR, Ser. Fiz., 47 (1983) 334.
81 M.E. Glicksman, S.R. Coriell and G.B. McFalden, Ann. Rev. Fluid Mech., 18 (1986) 307.
82 W.R. Wilcox, J. Cryst. Growth, 65 (1983) 133.
83 H.L. Swinney and J.P. Gollup, Hydrodynamic Instability and the Transition to Turbulence, Springer-Verlag, Berlin, 1981.
84 S. Carra, Progr. Cryst. Growth Charact., 11 (1985) 1.
85 S. Coriell, G.B. McFalden, R.F. Boisver, M.E. Glickeman and Q.T. Fang, J. Cryst. Growth, 66 (1984) 514.
86 Y. Yoo and B. Rubinsky, Int. J. Numer. Methods Eng., 23 (1986) 1785.
87 J.J. Favier and D. Camel, J. Cryst. Growth, 79 (1986) 50.
88 F. Rosenberger, Fundamentals of Crystal Growth I, Springer-Verlag, Berlin, 1979.
89 H.Y. Borchard and F. Daniels, J. Am. Cer. Soc., 79 (1957) 41.
90 M.M. Factors and R. Hanks, Trans. Far. Soc., 79 (1967) 1122.
91 J. Šesták, P. Holba and G. Lombardi, Ann. Chim. (Rome), 67 (1977) 73; Silikáty (Prague), 20 (1976) 83.
92 M. Nevřiva, P. Holba and J. Šesták, in E. Buzagh (Ed.), Thermal Analysis (Proc. 4th ICTA), Vol. 3, Akademy Kiyado, Budapest, 1974, p. 981; Silikáty (Prague), 20 (1976) 99.
93 P. Holba, M. Nevřiva and J. Šesták, Thermochim. Acta, 23 (1978) 213.
94 J. Šesták, Thermochim. Acta, 98 (1986) 339.
95 M. Nevřiva and J. Šesták, Thermochim. Acta, 92 (1985) 623.
96 A. Gaumann, Chimica, 20 (1966) 82.
97 A. Reisman, Phase Equilibria, Academic, New York, 1976.
98 A.R. Ubbelohde, The Molten State of Matter, Wiley, London, 1978.
99 I. Penkov and I. Gutzow, J. Mater. Sci., 19 (1984) 233.
100 P.F. James, Phys. Chem. Glasses, 15 (1974) 95.
101 E.G. Rowlands and P.F. James, Phys. Chem. Glasses, 20 (1979) 1.
102 J.J. Hammel, in A.C. Zettlemoyer (Ed.), Nucleation, New York, 1969.
103 D.R. Uhlmann, J. Am. Cer. Soc., 66 (1983) 95.
104 K.F. Kelton, A.L. Greer and C.V. Thompson, J. Chem. Phys., 79 (1983) 6261.
105 D.S. Kameneckaya, Kristallografiya, 12 (1967) 90.
106 D.E. Temkin and V.V. Shevelev, J. Cryst. Growth, 66 (1984) 380.
107 W. Studzinski, G.H. Spiegel and R.A. Zahoransky, J. Chem. Phys., 84 (1986) 4008.
108 A.K. Ray, M. Chalam and L.K. Peters, J. Chem. Phys., 85 (1986) 2161.
109 H. Rasmussen, J. Cryst. Growth, 64 (1983) 229.
110 R.A. Grange and J.M. Kiefer, Trans. ASME, 29 (1941) 85.
111 J. Lothe and G.M. Pound, J. Chem. Phys., 36 (1962) 2080.
112 M. Volmer and A. Weber, Z. Phys. Chem., 119 (1926) 227.
113 R. Becker and W. Döring, Ann. Phys., 24 (1935) 719.
114 J.B. Zeldovich, Zh. Eksp. Teor. Fiz., 12 (1942) 525.
115 J. Frenkel, Kinetic Theory of Liquids, Clarendon Press, Oxford, 1946.

116 F.F. Abraham, Homogeneous Nucleation Theory, Academic Press, New York, 1974.
117 D. Kashchiev, Surf. Sci., 18 (1969) 293.
118 W.J. Shugard and H. Reiss, J. Chem. Phys., 65 (1976) 2827.
119 D.T. Gillespie, J. Chem. Phys., 74 (1981) 661.
120 D. Kashchiev, Cryst. Res. Technol., 19 (1984) 1413.
121 D. Turnbull and J.C. Fisher, J. Chem. Phys., 17 (1949) 71.
122 Z. Kožíšek and Z. Chvoj, Non-stationary Crystallization in Simple Glass-forming Materials, Czech. J. Phys. 839 (1989) 1.
123 J.B. Zeldovich, Acta Physicochim., 18 (1943) 1.
124 F.C. Collins, Z. Elektrochem., 59 (1955) 404.
125 A. Kantrowitz, J. Chem. Phys., 19 (1951) 1097.
126 R.F. Probstein, J. Chem. Phys., 19 (1951) 619.
127 H. Wakeshima, J. Chem. Phys., 22 (1954) 1614.
128 J. Feder, K.C. Russell, J. Lothe and G.M. Pound, Adv. Phys., 15 (1966) 111.
129 A. Bruce and D. Wallace, Phys. Rev. Lett., 4 (1982) 457.
130 K. Binder, Adv. Coll. Interf. Sci., 7 (1977) 279.
131 D. Turnbull, Trans. AIME, 175 (1948) 774.
132 W.G. Courtney, J. Chem. Phys., 36 (1962) 2009.
133 F.F. Abraham, J. Chem. Phys., 51 (1969) 1632.
134 K.F. Kelton and A.L. Greer, J. Non-Cryst. Solids, 79 (1986) 295.
135 R.J. Schaefer and M.E. Glicksman, J. Crystal Growth, 5 (1969) 44.
136 I. Kanne-Dannetschek and D. Stauffer, J. Aerosol Sci., 12 (1981) 105.
137 D.Kashchiev, Surf. Sci., 22 (1970) 399.
138 Z. Kožíšek and Z. Chvoj, Crystal Res. Technol., 18 (1983) 307.
139 I.G. Bazhal, Kristallografiya, 14 (1969) 1106.
140 A. Yiabicki, J. Chem. Phys., 85 (1986) 3042.
141 J. Šesták, Thermochim. Acta, 110 (1987) 427.
142 A.N. Kolmogorov, Izv. Akad. Nauk SSSR, Otd. Mat. Estestv. Nauk., 3 (1937) 355.
143 J. Šesták, Phys. Chem. Glasses, 15 (1974) 137.
144 S. Ranganathan and M.V. Heimendall, J. Mat. Sci., 16 (1981) 2401.
145 J. Šesták, in D. Dollimore (Ed.), Proc. 2nd Europ. Symp. on Thermal Analysis, Heyden, London, 1981, p. 115.
146 J. Šesták and T. Kemeny, Thermochim. Acta, 110 (1987) 121.
147 T.Y.W. DeBruijn, W.A. DeJoung and D.J. van der Berg, Thermochim. Acta, 45 (1981) 315.
148 Z. Strnad, Glass Ceramic Materials, SNTL, Praha, 1982 (in Czech); Elsevier, Amsterdam, 1984.
149 D.R. McFarlane, J. Non-Cryst. Solids, 53 (1982) 61.
150 I. Gutzow, D. Kashchiev and I. Avramov, J. Non-Cryst. Solids, 73 (1985) 477.
151 R.W. Hooper, G. Scherer and D.R. Uhlmann, J. Non-Cryst. Solids, 15 (1974) 45.
152 D.R. Uhlmann, J. Am. Ceram. Soc., 66 (1983) 95.
153 J.S. Langer and A.J. Swartz, Phys. Rev. A, 21 (1980) 948.
154 D.R. Uhlmann, J. Non-Cryst. Solids, 7 (1972) 337.
155 D.R. Macforhene, J. Non-Cryst. Solids, 53 (1982) 61.
156 H. Reiss, J. Chem. Phys., 18 (1950) 840.
157 K. Binder and D. Stauffer, Adv. Phys., 25 (1976) 343.
158 D. Stauffer, J. Aerosol Sci., 7 (1976) 319.
159 R. Dhanasekaran and P. Ramasamy, Cryst. Res. Technol., 16 (1981) 1347.
160 R. Dhanasekaran and P. Ramasamy, Cryst. Res. Technol., 16 (1981) 863.
161 R. Dhanasekaran and P. Ramasamy, Cryst. Res. Technol., 16 (1981) 635.
162 V. Natarojan, C. Subramanian, D. Jayaromon and P. Ramasamy, J. Cryst. Growth, 79 (1986) 1001.

163 V.F. Razumov and A.J. Tarakanov, Inzh. Fiz. Zh., 49 (1985) 201.
164 J.P. Garnier, P. Mirabel and B. Migault, Chem. Phys. Lett., 115 (1985) 101.
165 G. Wilewski, J. Chem. Phys., 80 (1984) 1370.
166 R.G. Renninger, F.C. Hiller and R.C. Bone, J. Chem. Phys., 75 (1981) 1584.
167 J.S. Langer, Ann. Phys., 54 (1969) 258.
168 J.S. Langer and L.A. Turski, Phys. Rev. A, 8 (1973) 3230.
169 J.S. Langer and L.A. Turski, Phys. Rev. A, 22 (1980) 2189.
170 J.D. Gunton and M. Droz, Introduction to the Theory of Metastable and Unstable States, Springer, Berlin, 1983.
171 Z. Chvoj, Silikáty (Prague), 30 (1986) 103.
172 G.P. Ivantcov, Rost Kristallov III, Moscow, 1961, p. 75.
173 S. Krukowski and L.A. Turski, J. Cryst. Growth, 58 (1982) 631.
174 D.E. Temkin, Kristallografija, 28 (1983) 428.
175 E.A. Brener and S.V. Meškov, Kristallografija, 30 (1985) 461.
176 D.E. Temkin, Kristallografija, 28 (1983) 240.
177 E.A. Brener, V.I. Marčenko and S.V. Meškov, Zh. Eksp. Teor. Fiz., 85 (1983) 2107.
178 D.E. Temkin and V.V. Shevelev, Dokl. Akad. Nauk. SSSR, 253 (1980) 410.
179 D.E. Temkin and V.V. Shevelev, J. Cryst. Growth, 52 (1981) 104.
180 H. Trinhaus, Phys. Rev. B, 27 (1983) 7372.
181 D.E. Temkin and V.V. Shevelev, Kristallografija, 27 (1982) 1073.
182 D.E. Temkin and V.V. Shevelev, J. Cryst. Growth, 66 (1984) 380.
183 A.K. Ray, M. Chalom and L.K. Peters, J. Chem. Phys., 85 (1986) 2161.
184 Z. Chvoj, Kinetic Phase Diagrams in Processes of Nucleation, Czech. J. Phys. B, 38 (1988) 19.
185 Č. Bárta, Z. Pokorná, M. Rodová, J. Trnak and A. Tříska, Adv. Space Res., 6 (1986) 1.
186 A.A. Chernov, E.I. Givargizov, Ch.S. Bagdasarov, V.A. Kuznetzov, L.N. Demjanec and A.N. Lobachev. Sovremennaja kristallografija III, Obrazovanije kristallov, Nauka, Moscow, 1980.
187 J.C. Brice, The Growth of Crystals from Liquids, North-Holland, 1973.
188 D.E. Temkin, in Crystallization Processes, Consultants Bureau New York, 1966, p. 15.
189 J.W. Cahn and R. Kikuchi, Phys. Rev. B, 31 (1985) 4300.
190 A.D.J. Haymet and D.W. Oxtoby, J. Chem. Phys., 74 (1981) 2559.
191 D.W. Oxtoby and A.D.J. Haymet, J. Chem. Phys., 76 (1983) 6262.
192 V.T. Borisov, Dokl. Akad. Nauk. SSSR, 136 (1961) 583.
193 V.S. Yuferev, Poverkhn. Fiz. Chim. Mekh., 7 (1983) 29.
194 Z. Chvoj and P. Demo, The Basic Thermodynamical Equations of Surface Phases I, Proc. 4th ICSS, September 22–26, 1980, Cannes, France, Vol. 1, p. 15.
195 Z. Chvoj and P. Demo, Adv. Space Res., 1 (1981) 21.
196 P. Demo, Czech. J. Phys. B, 35 (1985) 715.
197 F. Vodák, Czech. J. Phys. B, 33 (1983) 930.
198 P. Demo, Czech. J. Phys. B, 36 (1986) 819.
199 J.W. Cahn, Acta Metall., 8 (1960) 554.
200 J.W. Cahn, J. Chem. Phys., 42 (1965) 93.
201 J.W. Cahn and R.S. Charles, Phys. Chem. Glasses, 6 (1965) 181.
202 W.K. Burton, N. Cabrera and F.C. Frank, Phil. Trans. Roy. Soc. London, A243 (1951) 299.
203 L. Onsager, Phys. Rev., 65 (1944) 117.
204 P. Bennema, J. Cryst. Growth, 69 (1984) 182.
205 K.A. Jackson, in Liquid Metals and Solidification, Ann. Soc. Met., Cleveland, 1958.
206 Jenn-Shing Chen, Nai-Ben Ming and F. Rosenberger, J. Chem. Phys., 84 (1986) 2365.
207 H. van Beijeren, Phys. Rev. Lett., 38 (1977) 993.
208 H.F.S. Knops, Phys. Rev. Lett., 39 (1977) 776.

209 W.R. Wilcox, J. Cryst. Growth, 7 (1970) 203.
210 A.A. Chernov, Zh. Eksp. Teor. Fiz., 53 (1967) 2090.
211 N.I. Stranski, Z. Phys., 119 (1942) 22.
212 N.I. Stranski, Naturwissenschaften, 30 (1942) 425.
213 N.I. Stranski, Naturwissenschaften, 31 (1943) 144.
214 R. Locmann and N.I. Stranski, J. Cryst. Growth, 13–14 (1972) 236.
215 T. Kurda and R. Locmann, J. Cryst. Growth, 56 (1982) 189.
216 J.Q. Broughton and G.H. Gilmer, J. Chem. Phys., 79 (1983) 5095.
217 J.Q. Broughton and L.V. Woodcock, J. Phys. C, 11 (1978) 2743.
218 A. Trayanov and D. Nenow, J. Cryst. Growth, 74 (1986) 375.
219 D. Nenow, in B.R. Pomplin (Ed.), Progress in Crystal Growth and Characterization, Vol. 9, Pergamon, Oxford, 1984.
220 V.I. Kolividze, V.F. Kiselev and L.A. Ushakova, Dokl. Akad. Nauk. SSSR, 191 (1970) 1088.
221 V.I. Kolividze, V.F. Kiselev, A.B. Kurzaev and L.A. Ushakova, Surf. Sci., 44 (1974) 60.
222 K.D. Stock and E. Menzel, J. Cryst. Growth, 43 (1978) 135.
223 K.D. Stock and E. Menzel, Surf. Sci., 61 (1976) 272.
224 H.H.G. Jellinek, J. Coll. Interf. Sci., 25 (1967) 192.
225 H. Heyer, F. Nietruch and I.N. Stranski, J. Cryst. Growth, 11 (1971) 283.
226 D. Beaglehole and D. Nason, Surf. Sci., 6 (1980) 357.
227 L.A.M.J. Jetten, H.J. Human, P. Bennema and J.P. van der Eerden, J. Cryst. Growth, 68 (1984) 503.
228 G.H. Gilmer, J. Cryst. Growth, 49 (1980) 465.
229 K. Kawasaki and T. Otta, Prog. Theor. Phys., 67 (1982) 147.
230 P. Bennema, J. Cryst. Growth, 69 (1984) 182.
231 G.H. Gilmer and P. Bennema, J. Appl. Phys., 43 (1972) 1347.
232 J.P. van der Eerden, P. Bennema and T.A. Cherepanova, Prog. Cryst. Growth Charact., 1 (1978) 219.
233 M. Ohara and R.C. Reid, Modeling Crystal Growth Rates from Solution, Prentice–Hall, New York, 1973.
234 J.W. Mullin, Crystallization, Butterworths, London, 1972.
235 J.A. Venables, G.D.T. Spiller and M. Hanbücken, Rep. Prog. Phys., 47 (1984) 399.
236 A.E. Nielsen, Kinetics of Precipitation, Pergamon, Oxford, 1984.
237 R. Kaischew, S. Stoyanov and D. Kashchiev, J. Cryst. Growth, 52 (1989) 3.
238 D. Kashchiev, J.P. van der Eerden and C. van Leewen, J. Cryst. Growth, 40 (1977) 47.
239 R. Dhanasekaran and P. Ramasamy, Cryst. Res. Technol., 16 (1981) 1339.
240 R. Dhanasekaran and P. Ramasamy, Cryst. Res. Technol., 16 (1981) 863.
241 C. Subramanian, R. Dhanasekaran, P. Ramasamy and D. Elwell, J. Cryst. Growth, 70 (1984) 41.
242 R. Dhanasekaran and P. Ramasamy, Cryst. Res. Technol., 16 (1981) 641.
243 F.C. Frank, Disc. Faraday Soc., 48 (1949) 67.
244 G.H. Gilmer, J. Cryst. Growth, 42 (1977) 3.
245 L.S. Griffin, Phil. Mag., 41 (1950) 196.
246 A.R. Verma, Phil. Mag., 42 (1951) 1005.
247 A.R. Verma, Cryst. Growth and Dislocations, Butterworths, London, 1953.
248 P. Bennema, J. Boon, C. van Leeuwen and G.H. Gilmer, Kristall Tech., 8 (1973) 659.
249 J.R. Garside, J. van Rosmalen and P. Bennema, J. Cryst. Growth, 29 (1975) 353.
250 W.S.P. van Enchevort and W.H. van der Linden, J. Cryst. Growth, 47 (1979) 196.
251 B. van der Hoek, L.A.M.J. Jetten and W.J.P. van Enchevort, J. Cryst. Growth, 62 (1983) 603.
252 P. Bennema and C. van Leeuwen, J. Cryst. Growth, 31 (1975) 3.
253 W. van Erk, H.S.G.J. van Hock-Martens and G. Bartels, J. Cryst. Growth, 48 (1980) 621.

254 F. Rosengerger, in B. Mutaftschiev (Ed.), Interfacial Aspects of Phase Transformations, D. Reidel, Boston, 1982, p. 315.
255 W.N. Mullins and J.P. Hirth, J. Phys. Chem. Solids, 24 (1963) 1391.
256 A.A. Chernov, Sov. Phys. Usp., 4 (1961) 116.
257 G.H. Gilmer, R. Ghez and N. Cabrera, J. Cryst. Growth, 8 (1971) 79.
258 P. Bennema, J. Boom, C. van Leeuwen and G.H. Gilmer, Kristall Tech., 8 (1973) 659.
259 G.H. Gilmer and P. Bennema, J. Appl. Phys., 43 (1972) 1347.
260 P.T. Cardew, J. Cryst. Growth, 60 (1982) 414.
261 A. Trayanov, Cryst. Res. Technol., 21 (1986) 175.
262 T. Sawada, J. Cryst. Growth, 60 (1982) 349.
263 B. Mutaftschiev, Crit. Rev. Solid State Sci., 6 (1976) 157.
264 D.E. Temkin, Sov. Phys. Cryst., 14 (1969) 344.
265 G.H. Gilmer, H.S. Leamy, K.A. Jakson and H. Reiss, J. Cryst. Growth, 24/25 (1974) 495.
266 G.H. Gilmer, J. Cryst. Growth, 42 (1977) 3.
267 U. Bertocci, J. Cryst. Growth, 26 (1974) 219.
268 G.H. Gilmer, J. Cryst. Growth, 35 (1976) 15.
269 Yu.A. Baikov, Yu.V. Zelenev and W. Haubenreisser, Phys. Status Solidi A, 59 (1980) k155.
270 Z. Chvoj, Cryst. Res. Technol., 21 (1986) 1003.
271 Z. Chvoj, Czech. J. Phys., B37 (1987) 1256.
272 Z. Chvoj, Cryst. Res. Technol., 8 (1986) 1003.
273 Z. Chvoj, Czech. J. Phys., B37 (1987) 607.
274 D.E. Temkin, Kristallografija, 21 (1976) 473.
275 D.E. Temkin, in Rost kristallov 13, Nauka, Moscow, 1980, p. 134.
276 E.A. Brener, Kristallografija, 32 (1987) 7.
277 S.E. Korshumov, Zh. Eksp. Teor. Fiz., 91 (1986) 1466.
278 Yu.D. Chistyakov, Yu.A. Baikov, H.G. Schneider and V. Ruth, Cryst. Res. Technol., 20 (1985) 1007.
279 Yu.D. Chistyakov, Yu.A. Baikov, H.G. Schneider and V. Ruth, Cryst. Res. Technol., 20 (1985) 1149.
280 Yu.D. Chistyakov and Yu.A. Baikov, Cryst. Res. Technol., 20 (1985) 1143.
281 G.H. Gilmer, Comput. Mod. Cryst. Growth Sci., 208 (1980) 355.
282 J.N. Cape and L.V. Woodcock, J. Chem. Phys., 73 (1980) 2420.
283 J.Q. Broughton, A. Bonissent and F.F. Abraham, J. Chem. Phys., 74 (1981) 4029.
284 C.L. Cleveland, U. Londman and R.N. Barnett, Phys. Rev. Lett., 49 (1982) 790.
285 G. Bushnell-Wye and J.L. Finney, Philos. Mag., A44 (1981) 1053.
286 R.J. Davey, J. Cryst. Growth, 34 (1976) 109.
287 U. Landman, Ch.L. Cleveland and Ch.S. Brown, Phys. Rev. Lett., 45 (1980) 2032.
288 J.Q. Broughton and G.H. Gilmer, J. Chem. Phys., 84 (1986) 5741.
289 J.Q. Broughton and G.H. Gilmer, J. Chem. Phys., 84 (1986) 5749.
290 J.Q. Broughton and G.H. Gilmer, J. Chem. Phys., 84 (1986) 5759.
291 A.M.J.G. van Run, J. Cryst. Growth, 54 (1981) 195.
292 Yu.D. Chistyakov, Yu.A. Baikov, H.G. Schneider and V. Ruth, Cryst. Res. Technol., 18 (1983) 6.
293 H. Pfeiffer and W. Haubenreisser, Phys. Status Solidi B, 96 (1979) 287.
294 H. Pfeiffer and W. Haubenreisser, Phys. Status Solidi B, 101 (1980) 253.
295 H. Pfeiffer, Phys. Status Solidi A, 72 (1982) 239.
296 H. Pfeiffer, Phys. Status Solidi A, 79 (1983) 445.
297 T.A. Cherepanova, A.V. Shirin and V.T. Borisov, Kristallografija, 22 (1977) 260.
298 T.A. Cherepanova, Prikl. Mekh. Tekh. Fiz., 5 (1978) 120.
299 T.A. Cherepanova, Prikl. Mekh. Tekh. Fiz., 6 (1978) 96.

300 T.A. Cherepanova and V.F. Kiselev, Kristall Tech., 14 (1979) 545.
301 T.A. Cherepanova and G.T. Didrihsons, Kristall Tech., 14 (1979) 1501.
302 T.A. Cherepanova and V.F. Kiselev, Kristallografija, 24 (1979) 327.
303 T.A. Cherepanova, in Rost kristallov TXIII, Nauka, Moscow, 1980.
304 T.A. Cherepanova, Phys. Status Solidi A, 58 (1980) 469.
305 T.A. Cherepanova, Phys. Status Solidi A, 59 (1980) 371.
306 T.A. Cherepanova, J. Cryst. Growth, 52 (1981) 319.
307 T.A. Cherepanova and A.S. Koziejowska, Phys. Status Solidi A, 77 (1983) 35.
308 T.A. Cherepanova and A.S. Koziejowska, Phys. Status Solidi A, 77 (1983) 561.
309 P. Gordon, Principles of Phase Diagrams in Material Systems, McGraw-Hill, New York, 1968.
310 V.M. Glazov and L.M. Pavlova, Chemical Thermodynamics and Phase Equilibrium, Metallurgiya, Moscow, 1981 (in Russian).
311 Yu.L. Klimontovitch, Statistical Physics, Nauka, Moscow, 1982 (in Russian).
312 Shang-keng Ma, Modern Theory of Critical Phenomena, Benjamin, London, 1976.
313 L.D. Landau and E.M. Lifshic, Statistical Physics, Nauka, Moscow, 1976 (in Russian).
314 F. Rosenberger, Fundamentals of Crystal Growth I, Springer-Verlag, Berlin, 1979.
315 P. Willars, J. Less-Common Met., 109 (1985) 93.
316 B.N. Rolov, Diffusive Phase Transitions, Zinatne, Riga, 1972 (in Russian).
317 Z. Chvoj, Czech. J. Phys., B28 (1978) 663.
318 V.Ye. Yegorushkin, V.Ye. Panin and Ye.V. Savushkin, Izv. Vyssh. Uchebn. Zaved. Fiz., 30 (1987) 9.
319 D.T. Gillespie, J. Chem. Phys., 74 (1981) 661.
320 D. Kashchiev, Cryst. Res. Technol., 19 (1984) 1413.
321 H. Metiu, K. Kitahara and J. Ross, J. Chem. Phys., 64 (1976) 292.
322 K. Binder, Monte-Carlo Methods in Statistical Physics, Springer-Verlag, Berlin, 1979.
323 A. Bruce and D. Wallace, Phys. Rev. Lett., 4 (1982) 457.
324 J.S. Langer and A.J. Swartz, Phys. Rev. A, 21 (1980) 948.
325 S.P. Delineshev and G.M. Bliznakov, Cryst. Res. Technol., 17 (1982) 1051.
326 S.P. Delineshev and G.M. Bliznakov, Cryst. Res. Technol., 17 (1982) 1323.
327 A. Milchev and K. Binder, Surf. Sci., 164 (1985) 1.
328 H. Müller-Krumbhaar, T.W. Burkhardt and D.M. Kroll, J. Cryst. Growth, 38 (1977) 13.
329 T.F. Meister and H. Müller-Krumbhaar, Z. Phys. B, 55 (1984) 111.
330 W.R. Wilcox, J. Cryst. Growth, 65 (1983) 133.
331 S.R. Coriell, G.B. McFadden, R.F. Boisvert and R.F. Sekerka, J. Cryst. Growth, 69 (1984) 15.
332 J. Keizer, J. Chem. Phys., 69 (1978) 2609.
333 H.L. Tsai and B. Rubinsky, J. Cryst. Growth, 69 (1985) 29.
334 S.R. Coriell and R.F. Sekerka, J. Cryst. Growth, 61 (1983) 499.
335 J. Kratochvíl, Cesk. Cas. Fys. (Prague), A36 (1986) 433.
336 M.E. Glicksman, S.R. Coriell and G.B. McFadden, Ann. Rev. Fluid Mech., 18 (1986) 307.
337 S.R. Coriell, G.B. McFadden and R.F. Boisvert, J. Cryst. Growth, 66 (1984) 514.
338 W.W. Mullins and R.F. Sekerka, J. Appl. Phys., 35 (1964) 444.
339 R.F. Sekerka, J. Appl. Phys., 36 (1965) 264.
340 B.Ya. Lyubov, Teoriya kristallizaciyi v bolshikh obyemakh, Nauka, Moscow, 1975.
341 J.S. Langer, Rev. Mod. Phys., 1 (1980) 1.
342 V.S. Yuferev, Poverkhn. Fiz. Chim. Mekh., 7 (1983) 29.
343 V.P. Skripov and A.V. Skripov, Usp. Fiz. Nauk, 128 (1979) 193.
344 A.D.J. Haymet and D.W. Oxtoby, J. Chem. Phys., 84 (1986) 1769.
345 A.D.J. Haymet, Prog. Solid State Chem., 17 (1986) 1.
346 B.B. Mandelbrok, The Fractal Geometry of Nature, Freeman, San Francisco, 1982.

347 D.S. Cannel and C. Aubert, Fractal and Non-Fractal Patterns in Physics, in H.E. Stanley and N. Ostrowski (Eds.), Growth and Form, Martinus Nijhoff, Dordrecht, 1986.
348 L.M. Sander, in F. Family and D.P. Landau (Eds.), Kinetics of Aggregation and Gelation, North-Holland, Amsterdam, 1984, p. 13.
349 S.H. Liu, Fractals and Their Applications in Condensed Matter Physics, in Solid State Physics, Vol. 39, Springer-Verlag, Berlin, 1986, p. 207.
350 V.S. Yuferev and E.N. Kolesnikova, Zh. Teor. Fiz., 52 (1982) 1285.
351 Wei Qing Jin and Hiroski Komatsu, Prog. Crystal Growth Charact., 11 (1985) 311.
352 A. Visintin, IMA J. Appl. Math., 35 (1986) 233.
353 C.E. Chang and W.R. Wilcox, J. Cryst. Growth, 21 (1974) 135.
354 T.W. Fu and W.R. Wilcox, J. Cryst. Growth, 48 (1980) 416.
355 H. Potts and W.R. Wilcox, J. Cryst. Growth, 73 (1985) 350.
356 R.J. Naumann, J. Cryst. Growth, 58 (1982) 554.
357 P.C. Sukanek, J. Cryst. Growth, 58 (1982) 208.
358 P.C. Sukanek, J. Cryst. Growth, 58 (1982) 219.
359 T. Jasinski, W.M. Roksenov and A.F. Witt, J. Cryst. Growth, 61 (1983) 339.
360 C.L. Jones, P. Capper and J.J. Cosney, J. Cryst. Growth, 56 (1982) 581.
361 P.S. Ravishankar and Ta-Wei Fu, J. Cryst. Growth, 62 (1983) 425.
362 R.J. Naumann and S.L. Lehoczky, J. Cryst. Growth, 61 (1983) 707.
363 C.J. Chang and R.A. Brown, J. Cryst. Growth, 63 (1983) 343.
364 J.M. Poate, J. Cryst. Growth, 79 (1986) 549.
365 R.F. Wood and G.A. Geist, Phys. Rev. B, 34 (1986) 2606.
366 T.A. Cherepanova, J. Cryst. Growth, 59 (1980) 371.
367 A.D. Solomon, V. Alexides and D.G. Wilson, SIAM J. Sci. Stat. Comput., 6 (1985) 911.
368 R. Ghez, J. Cryst. Growth, 19 (1973) 153.
369 W.A. Tiller and C. Kary, J. Cryst. Growth, 2 (1968) 345.
370 H.T. Meinden, J. Cryst. Growth, 6 (1970) 2218.
371 E.A. Brener and D.E. Temkin, Kristallografiya, 30 (1985) 243.
372 M.B. Geilikman and D.E. Temkin, J. Cryst. Growth, 67 (1984) 67.
373 A.M. Merjamov, Zadacha Stefana, Nauka, Novosibirsk, 1986.
374 D.G. Wilson, A.D. Solomon and P.T. Baggs, Moving Boundary Problems, Academic, New York, 1978.
375 L.I. Rubinstein, Problema Stefana, Zvayzgne, Riga, 1967.
376 Ch. Locharu and V.S. Yuferev, Isv. Akad. Nauk SSSR, Ser. Fiz., 47 (1983) 261.
377 A. Bezegh, L. Domokos and S. Gal, Cryst. Res. Technol., 18 (1983) 733.
378 V.S. Yuferev, Isv. Akad. Nauk SSSR, Ser. Fiz., 47 (1983) 261.
379 T.A. Cherepanova, Prikl. Mekh. Tekh. Fiz., 5 (1978) 120.
380 T.A. Cherepanova, Dokl. Akad. Nauk SSSR, 238 (1978) 162.
381 T.A. Cherepanova, Acta Crystall., Sect. A, 34 (1978) 209.
382 V.N. Kuzovkov, B.N. Rolov and T.A. Cherepanova, Izv. Akad. Nauk Latvian SSR, Ser. Fiz. Tekh., 5 (1977) 43.
383 V.N. Kuzovkov, B.N. Rolov and T.A. Cherepanova, Izv. Akad. Nauk Latvian SSR, Ser. Fiz. Tekh., 6 (1977) 15.
384 D.E. Temkin, J. Cryst. Growth, 52 (1981) 299.
385 T.A. Cherepanova, A.V. Shirin and V.T. Borisov, in Industrial Crystallization, Plenum, New York, 1976, p. 113.
386 T.A. Cherepanova, J.P. van Eerden and P. Bennema, J. Cryst. Growth, 44 (1978) 537.
387 J.P. van Eerden, P. Bennema and T.A. Cherepanova, Prog. Cryst. Growth Charact., 3 (1978) 219.
388 T.A. Cherepanova and V.F. Kiselev, Kristallografiya, 25 (1980) 327.
389 B. Caroli, C. Caroli and B. Roulet, J. Cryst. Growth, 66 (1984) 575.
390 V.V. Gagosov and V.A. Naletova, Fluid Mech. SSSR, 14 (1985) 93.

391 E.A. Brener and D.E. Temkin, Kristallografiya, 30 (1985) 243.
392 Z. Chvoj, Czech. J. Phys., B33 (1983) 961.
393 Z. Chvoj, Czech. J. Phys., B33 (1983) 1060.
394 Z. Chvoj, Czech. J. Phys., B34 (1984) 548.
395 Z. Chvoj and Č. Barta, Czech. J. Phys., B35 (1985) 532.
396 Z. Chvoj, Czech. J. Phys., B36 (1986) 863.
397 Z. Chvoj and Č. Barta, Czech. J. Phys., B36 (1986) 868.
398 Z. Chvoj, P. Přikryl and F. Vodák, Czech. J. Phys., B36 (1986) 1209.
399 Z. Chvoj, The Influence of Kinetics of Phase Transformation on the Constitution of the New Phase, in Communications on the MSE Study, MRS, Pittsburgh, 1986.
400 Z. Chvoj, Czech. J. Phys., B37 (1987) 1340.
401 K. Binder, Rep. Prog. Phys., 50 (1987) 783.
402 V. Ebeling, Obrazovaniye struktur pri neobratimykh processakh, Mir, Moscow, 1979.
403 P. Glansdorff and I. Prigogine, Thermodynamic Theory of Structure, Stability and Fluctuations, Wiley–Interscience, London, 1971.
404 T. Poston and I. Stewart, Catastrophe Theory and its Applications, Pitman, London, 1978.
405 W. Reier, Physica, 57 (1972) 565.
406 C.R. Willis and R.H. Picard, Phys. Rev. A, 9 (1974) 4343.
407 F. Shibata and T. Arimitsu, J. Phys. Soc. Jpn., 49 (1980) 891.